Theoretical Estimation of Cross Field Interaction in Plasma

by

Shahin Nasrin

Index No: **243/15/Phys./24**

A thesis submitted in partial fulfillment of requirements for the degree of
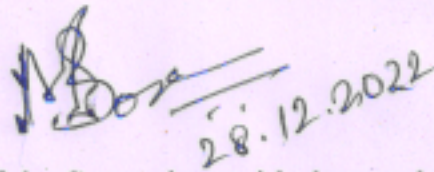***Doctor of Philosophy** (**Science**) at Jadavpur University.*

Department of Physics
Jadavpur University
Kolkata -700032

2022

Certificate from the Supervisor

This is to certify that the thesis entitled *"Theoretical Estimation of Cross Field Interaction in Plasma"* Submitted by Smt. **Shahin Nasrin** who got her name registered on 4th November, 2015 for the Award of Ph.D. (Sc.) degree of Jadavpur University, is absolutely based upon her own work under the supervision of **Professor (Dr.) Mridul Bose,** and that neither this thesis nor any part of it has been submitted for either any degree/ diploma or any other academic award anywhere before.

In my opinion, this thesis is fit for submission for the Ph.D. (Sc.) degree of Jadavpur University.

28.12.2022

(Signature of the Supervisor with date and official seal)

Dr. Mridul Bose
Professor of Physics
Department of Physics
Jadavpur University
Kolkata-700 032, India

Author's declaration

I declare that the work in this thesis was carried out in accordance with the requirements of the Jadavpur University's regulation and code of practice for research degree programme and that it has not been submitted for any other academic award. Except where indicated by specific reference in the text, the work is my own work. Any views expressed in the dissertation are those solely of the author.

Shahin Nasrin

Shahin Nasrin

Acknowledgement

I am indebted to my advisor Professor (Dr.) Mridul Bose for giving me the opportunity of doing research under him, and for all of his guidance and right advice throughout every step of this journey.

I am also greatly appreciative of the advice and direction provided by Dr. Salil Das parts of this research would have been nearly impossible without his involvement. Additionally, I am also thankful for all the support that the faculty members of the department of physics and the Ph.D. cell office stuffs have provided over the years.

I want to express my gratitude for the insightful conversations with Mr. Debashish Chattopadhya, Associate Professor at Vijaygarh College, Kolkata. Additionally, I';m grateful to Dr. Swapan Kr. Das for motivating me.

I must express my sincere appreciation to Dr. Phanishree from the University of Hyderabad, Ms. Nusrat Khan, research scholar from Barkatullah University, Mr. Avik Basu, Assistant professor of Raja Peary Mohan College, Dr. Agnita Kundu Assistant professor of Shri Shikshayatan College for their patience, unflagging support, and direction when I was feeling confused. Also, I'd like to thank Mr. Sakub Azam and Mr. Kinkar Dhara for their assistance with technical part during this journey.

Last but not the least, I'd like to express my gratitude to my parents Dr. Nurul Islam and Smt. Sahida Khatun, all my family members and some of my friends who always believed in me and shared my dreams.

Shahin Nasrin
(28/12/2022)

Dedicated to

Shamim Haque Mondal

List of publications

1.	**Nasrin, S**., Bose, M. (2022) Effect of two different electron temperatures in auroral ionosphere. Ukrainian Journal of Physics.,67(2),136 doi: 10.15407/ujpe67.2.136

Conference

1.	**Nasrin, S.,** Bose, M., (2019) Study of collisional plasma in presence of sheared magnetic field. In 12th International conference on plasma science, November 11, 2019, University of Lucknow, Lucknow, India.

2.	**Nasrin, S.,** Bose, M., (2018) Effect of Magnetic Shear on instability in collisional plasma. In 33rd National symposium on plasma science, December 07, 2018, Delhi University, Delhi, India.

3.	Das, S., **Nasrin, S**. and Bose, M., 2016, October. **EXB** instability with sheared magnetic field. In *APS Division of Plasma Physics Meeting Abstracts* (Vol. 2016, pp. YP10-096). Bibcode: 2016APS..DPPY10096D.

4.	**Nasrin, S**., Bose, M. (2016) Edge plasma transport in **EXB** configuration with sheared magnetic field., March 21, 2016, Jadavpur University, Kolkata, India

SYNOPSIS

Index No: 243/15/Phys./24

Title of Thesis: Theoretical estimation of cross field interaction in plasma

Plasma is an ionized gas where sufficient energy is provided to free electrons from atoms or molecules and to allow both ions and electrons to coexist. In order to understand the phenomena in a certain plasma region, it is necessary to map not only the magnetic but also the electric field. The interaction of these two fields in plasma produces a drift mode, the **E x B** drift which generally slowed down by neutral drag. The drifts cause asymmetries in the plasma equilibrium. The basic results can be understood by dividing the drifts into three categories diamagnetic, **E x B**, and **ΔB**. The dominant effect near the divertor plates is from the **E x B** drifts, while the weaker **ΔB** drifts cause an increase in the magnitude of the radial electric field. The study of such waves is important in magnetically confined inhomogeneous plasma devices because low frequency unstable drift wave instabilities reduce plasma confinement. On the other hand at plasma boundaries in upper atmosphere, lower hybrid drift waves (LHDWs) are often seen. The LHDW are mainly electrostatic current aligned waves, propagating perpendicularly to the ambient magnetic field. The free energy that drives these waves exists in density gradients and magnetic field gradients. Many studies of the LHDW have been done, both in space and in laboratory. In this thesis the investigations are concerned with the observation of drift waves in the low frequency domain. Here, we consider three different cross field interactions in different plasma regions.

The first problem consists of a finite density gradient and magnetic shear in a resistive domain where an analytical model of the **E x B** or drift instability for plasmas in plane slab geometry is proposed. A differential equation has been derived, gives an eigen mode which is shifted off the mode rational surface whereas the sheared magnetic field localizes the mode structure about the rational surface in the stabilized region. It is observed that magnetic sheared-driven stabilization of the growth rate occurs which is weakly dependent on the collision frequency at a smaller wavenumber region.

Here, in the second problem we have investigated the dynamics of waves that propagate in plasma of auroral ionosphere. The model we have consider contains stationary ions, cold electron fluid, neutrals, and hot electrons. Here, it has been shown that drift modes associated with lower-hybrid and electron-acoustic waves become stable under the influence of ion collisional damping by the cold electrons, but that unstable waves can develop when the electrons in the system are warm. At the same time it has been shown that lower-hybrid drift dissipative wave is not affected much in the presence of cold electrons. Finally, it means, that when the solar activity will very high the aurora generates in the higher latitude will affect more through the electron acoustic drift-dissipative mode.

In the third problem, momentum, trace impurity transport, and intrinsic rotation in tokamaks is trying to be studied using an electrostatic, collisionless fluid model for ion-temperature-gradient and trapped-electron mode driven turbulence in presence of radio frequency fields in the lower hybrid range of frequencies. The four-wave parametric process involving a lower hybrid source wave and ion temperature

gradient (ITG) mode and lower hybrid sidebands, respectively, are considered. Explicit expressions for the non-linear growth rate and the associated ion thermal conductivity are derived. The parametric coupling between the pump wave and ITG produce sideband waves in the lower hybrid range of frequencies are trying to be studied. The pump and the sidebands exert a ponderomotive force on electrons, modifying the eigenfrequency of the drift wave and influencing the growth rate.

Full Signature of the Candidate

Shahin Nasrin

(Shahin Nasrin)

Full Signature of the Supervisor

28.12.2022

Dr. Mridul Bose
Professor
Dept. of Physics
Jadavpur University

Index

List of figure

Abbreviation

TDE	**T**hermodynamic **E**quilibrium
MHD	**M**agneto-hydrodynamics
PDE	**P**artial **D**ifferential **E**quation
FAC	**F**ield **A**ligned **C**urrent
EUV	**E**xtreme **U**ltraviolet
EAW	**E**lectron-**A**coustic **W**ave
ITG	**I**on **T**emperature **G**radient
FLR	**F**inite **L**armor **R**adius

Symbols Used

c	Speed of light in vacuum
e	Electron charge
M	Mass of the ion
Ω_i	Ion cyclotron frequency
ω	eigen frequency
ν	collision frequency
k	wave vector
γ	growth or damping rate
λ	Mean free path
$\hbar$	Reduced Planck's constant
ρ_i	Ion Larmor radius
s	Magnetic shear
L_n	Density scale length
L_s	Shear scale length
q	Safety factor
η	Ion Temperature Gradient

"Stability isn't nearly so spectacular as instability"

......*Aldous Huxley from "**The Brave New World**"*

Chapter 1

Introduction

Plasma physics is the study of collective processes in many-body systems of charged particles. To understand the phenomena occurring in different fields such as astronuclear physics, solar physics, atmospheric physics, condensed matter physics and molecular biology, and many more we need to study the subject thoroughly. It is based on some well-established principles at the microscopic level. In case of plasma physics, the descriptions based on fluid equations consider self-consistent moments of the electrons and ions, whereas, for kinetic equations, Maxwell's distribution functions in multidimensional phase space are considered. The plasma state is characterized by the existence of a multitude of collective motions over a very wide range of spatial and temporal scales. The interaction of these collective movements often results in turbulence or coherent patterns and structures. A priori theoretical prediction of plasma behavior has achieved only limited success. Therefore, experiments are critical to the identification of fundamental processes in plasma, such as the evolution of coherent structures arising from nonlinear interactions. These interactions form the building blocks for understanding the evolution of complex processes.

The history of plasma science is as diverse as the subject itself. In the early days in the laboratory, plasma science is described, beginning with the work of Faraday in

the 1830's on the chemical transformation of the elements and continuing with Langmuir's work on gas discharges in the 1920's and research on electron beams and beam-type microwave devices in the 1940's and 1950's. Within a decade of Langmuir's work, the discovery of a fact that radio waves reflect from the ionosphere established the existence of the space plasma that surrounds the Earth. A new era in plasma physics began with the international development of efforts to achieve controlled thermonuclear fusion in the 1950's and with the space program. For the past few years, space, fusion, and the development of advanced weapons systems have been the main drivers for plasma science research [1].

Previously fundamental theories of plasma waves had concentrated on relatively straightforward issues like the propagation of waves in stationary homogenous plasmas with infinite extent. Maxwell's equations and other linearized partial differential equations (PDEs) describe the plasma response that can be applied to these ideal instances to study wave physics by applying the conventional Laplace and Fourier transformations [2]. However, dealing with real-world issues is undoubtedly more difficult; for instance, waves typically travel through inhomogeneous plasmas, are susceptible to mode conversion, and are affected by nonlinear events. Using conventional analytical methodologies, it becomes difficult or even impossible to describe the dynamics of waves in these non-ideal conditions.

 Waves play a different role in many aspects of plasma dynamics, and they are also essential for the handling and diagnostics of plasmas [2, 3]. In the particular context of magnetic confinement, several important applications of waves including plasma

heating [4] current drive [5, 6] mode stabilization [7, 8] etc. represent important developments in the mission of obtaining consistent nuclear fusion energy. Although several works have been done in the field of these and other plasma-wave effects in the past, the area is still full of challenges and opportunities.

A wide range of fundamental configurations and phenomena were studied at the outset of the fusion and space programs. The achievement of fusion plasma conditions in the laboratory is a consequence of fusion research evolved to focus on systems with the minimum complexity. Inertial fusion research evolved in directions that either minimized nonlinear laser-plasma interactions or optimized particle-beam drivers. Magnetic fusion research concentrated on the tokamak approach, which is the most stable asymmetric confinement configuration. The principal difficulty encountered in fusion has been the inability to predict the nonlinear behavior of plasmas to the accuracy required by engineering considerations.

In the exploration of space plasmas, it was not possible to reduce the natural complexity of the magnetic field geometry through engineering design. Spacecraft data have identified many key nonlinear phenomena: collisionless shocks and steady magnetic reconnection, double layers, current sheets, dynamo generation of magnetic fields, and the overall structure of magnetospheric plasmas, which are high-mirror-ratio magnetic confinement configurations because, only the elementary aspects of these processes have been measured by spacecraft obtained local data [9].

While the discoveries of plasma phenomena in the space environment are remarkably varied, their abstractions into basic plasma processes are subject to

investigation by numerical computation, laboratory experiments, and analytical theory. One can anticipate that plasma phenomena discovered through spacecraft and astronomical observations, as well as in fusion research, will play an important role in laboratory experimentation.

Technological advances promise to create fundamentally new classes of plasma experiments and enable new diagnostics. Our conceptual understanding of plasma dynamics will be enriched by a theoretical explanation of the visualization techniques.

1.1 Forces on Plasma

The various types of forces control the dynamical behaviour of charged particles, both in the laboratory and space plasmas such as the electromagnetic force, gravitational force, ion drag force, ponderomotive force, etc. The electromagnetic force is the combined effect of the electric and magnetic fields. On a moving charged particle with charge 'q' and velocity, $\vec{v}$ the ***Lorentz force*** is given by,

$$\vec{F}_{EM} = q(\vec{E} + \vec{v} \times \vec{B}) \tag{1.1}$$

The Lorentz force acts in opposite directions on electrons and ions but the force on non-electrical origin acts in the same direction on all particles so, the effect of this force drag all charged particles in the same direction.

The ***gravitational force*** arises due to massive dust grains and ions. The motion of large celestial bodies are generally governed by the influence of gravitational force whereas the motion of charged particles is affected by electromagnetic force. There are some different micron and submicron-sized particles where both the

4

electromagnetic and gravitational forces are equipotent and referred to as ***gravito-electrodynamics*** [10].

The ***ion drag force*** is due to the relative motion between the charged particles, dust, and neutrals in the multicomponent plasmas. The ***thermophoretic*** force is associated with the temperature gradient of neutral gas particles and radiation pressure force. The ion drag force consists of two parts, namely the collective and the orbital forces. The collective force is associated with the momentum transfer from the ions that are collected by the grains, whereas the orbital force is due to the momentum transfer from ions that are scattered from the electric field of the grain.

Light waves exert a weak radiation pressure which is hard to detect. When high-powered microwaves or laser beams are used to heat a confined plasma, the force is coupled to the particle in a very subtle way and is called the ***ponderomotive force***, and its expression is given by,

$$\vec{F_p} = -\frac{\omega_{pe}^2}{\omega^2} \vec{\nabla} \left(\frac{<\varepsilon_0 E^2>}{2}\right) \tag{1.2}$$

$\vec{F_p}$ is mainly acting on the electrons but the effect is also transmitted to the ions due to its low frequency.

1.2 Plasma Instabilities

When all of the forces acting on a system are in balance and a steady-state solution is feasible for that equilibrium state, the system is said to be in equilibrium. Even though all the forces are in balance, the situation might not be in thermodynamic equilibrium (TDE). Any statistical system in TDE will tend to occupy the lowest potential energy

state, thus gaining higher stability. If a plasma is made to depart from TDE by some internal or external agent, thereby reducing its stability, free energy may be available. An instability thus ensues to bring the plasma to a lower potential energy state, hence closer to stability. If the instability grows either spatially or temporally, then it is said to be unstable. On the other hand, if it dampens it is said to be stable. Whatever instability develops or reduces depends on several variables, including the nature of the drivers and how they change as well as the plasma state at that precise moment in time and space. Plasma instabilities can be divided into two primary groups depending on the area of interest as follows [11].

Configuration Space or Micro Instabilities

Here we take into account the instabilities in the fluid domain. The plasma is considered a macroscopic entity and the departure from an equilibrium of its macroscopic variables is analyzed. The MHD equations are used and normal mode analysis is usually successful. The Maxwellian velocity space departures are neglected.

Velocity space or Macro Instability

Here we work in the kinetic domain and hence modification of Maxwellian velocity distribution is considered. Their analysis is much more complicated than the Macro Instabilities. Perturbation techniques are applied to the equations of the kinetic theory to analyze these instabilities.

Perturbation methods are usually employed to study plasma instabilities. Some variables may be perturbed while other variables are fixed or some variables may be

perturbed simultaneously. The resulting instability is analyzed theoretically using the normal mode method. Normal Mode analysis uses perturbation techniques. It gives complete information about the instability including its growth rates, which is a measure of how fast the instability grows or dampens. This method requires the plasma equation to be completely solvable which may be impossible in many cases. The theoretical study of plasma can be divided into three domains. The first one – is the most precise and idealistic, which is the impossible domain. We need to follow the trajectories and continuously calculate the effect of every particle's electric and magnetic fields on every other particle. The next accurate domain is the kinetic domain, where beautiful spatial and velocity distribution functions are used to follow the temporal and spatial variations of the plasma. Departures from the stable Maxwellian distribution are treated with the due mathematical process. The third domain is the fluid domain, though it is not as accurate as the kinetic domain [9] about 80% of the observed phenomena can be explained in this domain. We no longer recognize the individual particles of the plasma but treat the plasma as a fluid element. Hence the dependent variables of this fluid are now only a function of four independent variables (x, y, z, t) and reduce the mathematical complexity. The starting equations used in the fluid approach are called transport equations and are obtained by taking moments about the ***Boltzmann equation*** with a suitable distribution function. Whatever the domain, the plasma is acted upon by forces both electromagnetic and mechanical, and by making some assumptions and restricting the solution to certain domains, one can understand the underlying physics of the instability and get an estimate of its growth rate, stability domains, etc.

1.3 Cross Field Instabilities

Cross field instabilities are among the most studied phenomena in plasma physics driven by gradients in the plasma pressure, they are one of the "universal" instabilities that can arise in plasma [1]. From early studies in the 1960's [12], it has been shown that the generation of drift waves in collisional plasmas can lead to enhance plasma transport. Similar work [13] using a modulated electron current along the magnetic field lines showed it is possible to stabilize the drift waves and, in turn, improve plasma confinement. While early studies of drift instabilities were performed in linear plasma devices, the physical mechanism of drift instabilities is pervasive across all plasma experimental geometries. In particular, the edge region of fusion devices, where large density gradients are often established, is believed to be dominated by drift wave-driven turbulence [14, 15, 16]. In periods when the drift wave instability amplitude is large, there can be significant cross-field transport and enhanced plasma losses [13, 17, 18]. However, when large flows exist in the edge region whether established by self-consistent zonal flows or driven by external electrodes, there can be a significant reduction in drift wave turbulence. It was noted that the drift waves' amplitude grew with increasing shear length but eventually stabilized after the shear length reached a critical point [17].

These studies demonstrate how current research on fundamental plasma devices can yield different perspectives on basic physics. This study presents many observations of drift instabilities caused by plasma flows parallel to the magnetic field in fusion devices and space.

1.4 Brief Introduction of the Thesis

In this thesis, the investigations are concerned with the observation of drift waves in the low-frequency domain. Here, we consider three distinct cross-field interactions in various plasma regions. We start the second chapter with a general theoretical framework of $\mathbf{E} \times \mathbf{B}$ briefly so that readers can get an overview of the next chapters quickly.

In the third chapter, a study of a problem involving magnetic shear and a finite density gradient in a resistive domain is presented, along with a proposal for an analytical model of the $\mathbf{E} \times \mathbf{B}$ or cross field drift instability for plasmas in plane slab geometry. In contrast to how the sheared magnetic field localizes the mode structure about the rational surface in the stabilized zone, a differential equation has been constructed that yields an eigen mode that is shifted off about the mode rational surface. At a smaller wave number regime, it is seen that the growth rate stabilizes due to magnetic shearing, which weakly depends on the collision frequency only.

We have looked into the dynamics of waves that travel through the plasma of the auroral ionosphere in this fourth chapter. We have taken into account a model with stationary ions, neutrals, hot electrons, and cool electrons. Here, it has been demonstrated that drift modes linked to lower-hybrid and electron-acoustic waves stabilize under the effect of ion collisional dampening by the cold electrons, however unstable waves might emerge when the system's electrons are warm. In addition, it has been shown that the presence of cold electrons has little impact on the lower-hybrid drift dissipative wave. Finally, it means that the electron acoustic drift-

dissipative mode will have a greater impact on the aurora generated in the lower latitude when solar activity is very strong.

In the fifth chapter, momentum, trace impurity transport, and intrinsic rotation in tokamaks are investigated by using an electrostatic, collisionless fluid model for ion-temperature-gradient and trapped-electron mode-driven turbulence in the presence of radio frequency fields in the lower hybrid range of frequencies. Lower hybrid sidebands and a pump wave with an ITG (η_i) mode make up the four-wave parametric process. We derive an expression for linear dispersion relation. Nonlinear growth rate in the lower hybrid range of frequencies, still has to be examined, sideband waves are produced by the parametric coupling of the pump wave and ITG. The ponderomotive force that the pump and sidebands apply to electrons changes its number density, the drift wave's eigenfrequency. The perturbed densities of the electron and ion side bands is calculated in this chapter. Finally we summaries the whole work in the sixth chapter with a discussion and possibilities of the research.

Chapter 2

A Theoretical Approach to Study
E × B Drift Instability

Plasma is an ionized gas in which sufficient energy is provided to release electrons from atoms or molecules and allow both ions and electrons to coexist. To understand the phenomena in a certain plasma region, it is necessary to understand not only the magnetic but also the electric field. The interaction of these two fields in the plasma creates a drift mode, the **E × B** drift.

In plasmas, a large number of drift-type modes driven by *density and/ or temperature gradients* are expected to be unstable. Drift modes driven by trapped electrons and the ITG have been the subject of extensive theoretical investigations because of their relatively large growth rates and long wavelengths. In tokamaks and other magnetic confinement devices, various drift-type instabilities driven by pressure gradients can occur over a wide range of crossed-field wavelengths. Numerous dimensionless parameters characterize a tokamak discharge, including s (*magnetic shear*), q (*safety factor*), L_n (*density gradient length*) *β factor*, *inverse aspect ratio*, and many more. In drift stability analysis, the dependence of the growth rates on those parameters are of primary interest, as it may open a new direction to stabilization.

In addition to having a single mode, drift waves also include turbulent dynamics, which means that several modes interact nonlinearly. Due to its influence on anomalous transport, drift-wave turbulence is of great interest. It would seem logical

to believe that regulating drift-wave dynamics would also manage fluctuation-induced transport. Therefore, active control of the turbulent dynamics of drift waves is of great interest to improve plasma confinement in magnetic fusion devices.

2.1 Review of Research Work

The drift instability is the most promising choice for causing anomalous transport at the plasma boundary. In magnetized plasmas, many collective modes may be present, but the lowest frequency mode $\omega \ll \frac{eB}{M_i c} \ll \omega_{ci}$ controls transport. At these low frequencies, the ion-acoustic oscillations are determined by the parallel component of the wave vector $(k_\parallel)$, and the perpendicular component $(k_\perp)$ associated with the electric field which produces the $\mathbf{E} \times \mathbf{B}$ drift of the particle guiding centers across the magnetic Field [19] which are predominantly electrostatic. The fluctuations caused by drift wave affect plasma density and potential, and occur in the low-frequency region much below the ion cyclotron frequency.

Theoretical studies of drift mode in magnetically confined plasmas have a long history. The first study of the drift instability was based on a local analysis in the shearless slab geometry in which the wavenumber parallel to the ambient magnetic field, is constant and properly defined. Later, a methodology for non-local analysis [20] [21] in shear plate geometry was developed and a condition for suppressing instability due to magnetic shear was found. More rigorous analyzes showed that the drift mode in a shear plate geometry should be very stable even under weak magnetic shear [22] [23]. However, in the toroidal-induced drift mode [24], shear stabilization

is unable to overcome the destabilization it produces. The plate mode [22] [23] remains stable in toroidal geometry.

Recent research on plasma confinement has shown that the main factor controlling plasma transport through the magnetic field is low-frequency drift wave fluctuations. The first experimental observation of drift waves is made by D Angelo et al. in the early 1960s [25]. The first theoretical work was done by Moiseev and Sagdeev [26] and Jukes [27]. Thereafter, the importance of microscopic physical processes and the universal character was recognized. Very soon Chen and Lashinsky [28] [29] [30] recognized the importance of microscopic physical processes and their universal character. Here, linearized local slab models were used [29] [31] [32] in which the cylindrical geometry of the laboratory plasma was replaced by local Cartesian coordinates. A few years later, the first non-local cylindrical models assuming Gaussian density profiles were used to improve the theory [33]. Ellis, Marden-Marshall, and their co-workers [15] [34] showed that non-local cylindrical models give quantitative agreement between experiment and theory. It is important to consider the static radial electric field and the resulting $\mathbf{E} \times \mathbf{B}$ rotation of the plasma column [35].

Drift waves also occur at the edge of high-temperature fusion plasmas, where experimental access is sometimes limited [23] [36]. Moreover Low-temperature plasmas with cylindrical geometries allow the study of drift waves without electrons due to curved and inhomogeneous magnetic fields presented in toroidal geometries. In a word, Drift instability has been studied in many different plasma parameter

regimes accessible in linear devices, including collisionless [37] as well as collisional [31] plasmas, weakly ionized [38] as well as fully ionized plasmas [31]. In the above discussion, most of the experimental work on drift waves in laboratory plasmas has been done in plasmas with low β, i.e. the ratio of plasma pressure to magnetic-field pressure is much less than the electron-ion mass ratio m_e/ M_i, where, m_e is the mass of the electron and M_i is the mass of the ion.

Since the late 1960s, attempts to control drift-wave dynamics and the associated transport have been made where feedback techniques were used to suppress single drift modes [38] [39]. Usually, fluctuations were recorded, phase-shifted, amplified, and fed back into the plasma via electrodes. Alternatively, modulated microwaves at low power were used to suppress drift waves [40]. The confinement could be improved by suppression of fluctuations, but each drift mode requires separate feedback parameters for suppression. Consequently, it was not possible to achieve suppression of broadband fluctuations. Promising results in fusion devices have been obtained with biasing techniques that suppress turbulence through a shear flow [41].

2.2 Plasma Models

Plasma is a very complicated system with magnetized or unmagnetized plasma medium due to the presence of several effects, such as, presence of several kinds of species, e.g. two temperature electrons, positive ions, negative ions, and beam ions. Along with the existence of dissipative like collision, viscosity.

The basic system of equations governing the plasma dynamics can be written considering these effects, both in the kinetic model approach and the fluid model

approach. All these techniques exhibits take an important role in the formation of various nonlinear equations and all nonlinear phenomena can be studied by both the above-mentioned approach. Again due to the various types of charged particles in unmagnetized plasma, there exist several kinds of waves, like electron acoustic waves, and ion-acoustic waves, whereas ***Alfven waves*** and ***magnetosonic*** waves occur in magnetized plasma. But due to the complexity of the plasma dynamics, it is impossible to understand all these effects in a single physical model. Therefore, it is a general idea to develop various models by considering only a few of these effects at a time so that an evaluation of nonlinear equations can be derived for these waves.

2.3 Mathematical Framework behind Drift Instability

In the fluid approximation, the plasma is assumed to consist of two or more interacting liquids, for each type of particle. Plasma parameters such as density, velocity, and temperature of each species are introduced in the fluid equations, which are the statistical moments of the kinetic equations. The most simplifying picture is magneto-hydrodynamics where the plasma is treated as a single fluid. Drift waves must be described in the two fluid pictures of plasma because the electron and ion dynamics have to be treated separately. The basic equations used in the fluid model comprises of the continuity equation, the momentum equation, and Maxwell's electromagnetic equations.

Basic Fluid Equations

2.3.1 The continuity equation

This equation follows from the conservation of mass, which says that the change in the number of particles in a fixed volume depends on the net flux of the particles across the surface bounding that volume and also depends on any sources or sinks present inside that volume. It is given by the following equation where P_α' is the production rate and L_α is the loss rate of the species α.

$$\frac{\partial n_\alpha}{\partial t} + \vec{\nabla}(n_\alpha v_\alpha) = P_\alpha' - n_\alpha L_\alpha \tag{2.1}$$

2.3.2 The Momentum Equation

This equation follows from the conservation of momentum or the equation of motion. It is given by the following equation for the species α.

$$n_\alpha m_\alpha \left[\left(\frac{\partial}{\partial t} - u_\alpha \vec{\nabla}\right) u_\alpha\right] + \vec{\nabla} p_\alpha - n_\alpha m_\alpha \vec{g} + \vec{\nabla}\,\vec{\tau} - n_\alpha e_\alpha \left[\vec{E} - \vec{u_\alpha} \times \vec{B}\right]$$

$$= n_\alpha m_\alpha \sum v_{\alpha\beta}\left(\vec{u_\alpha} - \vec{u_\beta}\right)$$

$$\tag{2.2}$$

The first term in the left-hand side of the equation (2.2) is the convective derivative term which, represents the change in the velocity in a frame moving with the fluid. The second term represents the pressure gradient force, the third term represents the gravitational force, the fourth term is the stress force, and the final term is the Lorenz force. In the right-hand side $v_{\alpha\beta}\left(\vec{u_\alpha} - \vec{u_\beta}\right)$, represents the collision forces of the species with all other species.

16

2.3.3 Equation of state

From thermodynamics this can be written as,

$$P = c\rho^{\gamma}$$

Taking gradient on both side we get the most commonly used form

$$\vec{\nabla}P_{\alpha} = k\gamma T_{\alpha}\vec{\nabla}n_{\alpha}$$

Here α is denoting the different species present in plasma, γ is the specific heat capacity ratio of the species. P and n represents the pressure and number density.

2.3.4 Electromagnetic Equations

These are the four Maxwell's equations along with the Lorenz electromagnetic force (mentioned earlier) used in fluid model analysis.

$$\nabla.\vec{E} = 4\pi e(n_i - n_e) \tag{2.3a}$$

$$\nabla.\vec{B} = 0 \tag{2.3b}$$

$$\nabla \times E = \frac{1}{c}\left(4\pi\vec{j} + \frac{\partial\vec{E}}{\partial t}\right) \tag{2.3c}$$

2.4 Procedure for Deriving the Growth Rate

The following section gives a brief outline of the various steps to be followed to get an expression for the growth rate. Linear perturbation techniques are employed together with various assumptions and of course mathematical wizardry. I refrain from a detailed derivation since each expression for the growth rate is unique and

contains many intermediate steps. It is not instructive to try and derive all of them, however, the following steps are common in most derivations.

Step1. Equations (2.3a) through (2.3c) are first simplified by adapting them according to the region of interest. For example, in our situation, we will be using them in fusion devices as well as in the high-latitude F region where plasma transport dominates over either production or loss processes. So, in the continuity equation (2.1), we can neglect the production and loss terms on the right-hand side depending on particular situation.

Step 2. Assumptions are made to simplify the problem. By making assumptions we solve the problem in various domains or regions. For example, instead of using an arbitrary orientation of the electric field, which is the realistic case, we may choose to concentrate on the component of the electric field that is perpendicular to the density gradient. By doing this we now have to worry about only one component of the electric field instead of solving for all three components. This step is probably the most important. In further sections where we will be using the different growth rate expressions, we will try to justify the assumptions made to arrive at that expression.

Step 3. The plasma parameters are perturbed about their equilibrium values (mostly fixed in the previous step). For example. The electron density 'n' can be replaced by $= n_0 + n'$, where n_0 is the equilibrium density and n' is the perturbed density.

Step 4. Linearize the perturbed equations, i.e., neglect all second-order terms. This ensures that the problem does not spill over to the nonlinear domain, which makes it so much easier to solve. For example, we can neglect terms e.g. $n_i E_i$, n_i^2, v^2, etc,

where ν is the collision frequency Otherwise, it might be impossible to solve them in the nonlinear domain..

Step 5. Assume plane wave solutions, i.e., apply only sinusoidal perturbations. For example, the density perturbation is $n = n_0 \exp i(kx - \omega t)$. This assumption will allow us to replaced $\frac{\partial}{\partial t}$ with $-i\omega$ and $\vec{\nabla}$ with $-i\vec{k}$.

Step 6. Solve the set of simultaneous linear equations and get the dispersion relation.

Step 7. Find the roots of the dispersion relation which gives $\omega = \omega_r \pm i\gamma$. The growth rate is the imaginary part of ω. If any or all of the ω's have positive imaginary parts, the perturbation grows in time. Negative imaginary roots indicate damping and stability.

The procedure outlined above has been used by the author in deriving the different growth rate expressions.

2.5 Discussion

We can treat the plasma system as a hydrodynamic fluid when the mean free path (λ) of its particles is small compared to the scales of interest to have well-defined values of macroscopic parameters like density ρ(x, t), velocity v(x, t); pressure P(x, t); and anything else that is relevant, e.g. magnetic field. When we assumed the velocity distribution to be Maxwellian in the derivation of the problems presented in the next two chapters, we did implicitly imply that there were collisions. Frequent collisions lead to such distribution in most cases. As a result, although there are some situations where these deviations are significant, the fluid theory is not particularly sensitive to

variations from the Maxwellian distribution and we miss some important physics in plasma. The magnetic field, when present, in some ways imitates collisions, which is another reason why the fluid model accounts for plasmas.

Chapter 3

Study of E × B Instability for Ions under Influence of Sheared Magnetic Field

The cross-field (**E** × **B**) instability sometimes is called gradient drift instability. This instability was started to be investigated primarily for the laboratory discharge plasma experiments [42] [43]. Later it was extended to fusion devices, space, and astrophysical plasmas. For the stabilization at high-temperature plasmas in nuclear devices, the effect of magnetic shear is studied broadly for both collisional and collisionless plasmas [44] [45]. It has been shown from different research work that the sheared magnetic field has two effects that can stabilize the drift instabilities either by an effective increase in ion landau damping through different ways, like wave-packet propagation and expansion of potential well into the region where the interaction of the ion with landau damping is strong or by shortening the localized region of the wave packet until it vanishes [46]. Drift wave instabilities decrease the plasma confinement in a tokamak by enhancing the cross-field transport of particles and energy. The reduction in transport was due to an increase in the sheared flows in the plasma [47]. If a shear flow layer developed in the edge region of the plasma, its density increases. As a result, there was a decrease in overall electrostatic fluctuations and particle transport [48], [49]. Also, **E** × **B** flows lead to a reduction of electrostatic fluctuations in the shear region, which in turn reduces the particle flux and transport in the plasma. In different experiments, it was observed that **E** × **B** flows lead to a

reduction of electrostatic fluctuations in the shear region, as well as the particle flux and transport in the plasma [50].

The main cross-field modes appear to give rise to several other modes possibly through nonlinear wave-wave interaction which plays an important role in the saturation of the cross-field instability [51]. These modes exist in frequency regimes that extend from well below the ion cyclotron frequency up to the lower hybrid frequency [36]. In linear and nonlinear theories of drift waves, magnetic shear plays an important role to measure the fluctuations. The shear stabilization criteria for collisionless drift waves are obeyed in L-mode [52]. When the collisional effect increases it broadens the mode and enhances the electron damping. On the other, if the shear weakens, the electron damping increases, whereas the effect of ion damping deteriorates [53]. The effect of shear on resistive drift modes are studied for ionosphere and fusion devices earlier for the stability analysis in long wavelength as well as short wavelength range [36]. The behavior or cross-field current-driven ion acoustic instability is investigated theoretically in presence of sheared magnetic field and density gradient under a condition that shear damping dominates over landau growth and the critical shear length was found to be varied as $\sqrt{\frac{m_i}{m_e}}$ and $\left[\frac{V-c_s}{c_s}\right]^{-\frac{2}{3}}$ where V is the motion of the ions and $c_s = \frac{\omega}{k}$ [54]. Experimentally the effect of magnetic shear on stability is also studied by many researchers. The study of shear stabilization of drift dissipative instabilities taking into account the collisional effect and axial ion motion for hydrogen plasma found that, in presence of shear the waves maintain drift wave structure, and the radial mode is the lowest-order normal mode [55]. Also Chang

et al. [56]. Studied collisional, electrostatic drift waves, driven solely by diamagnetic currents with magnetic shear and destabilized by a positive electron temperature gradient which produces localized drift eigenmode near the mode rational surfaces for magnetic shear limit $\frac{L_n}{L_S} = 0.5$ [57]. Other collision-less and collisional drift modes become stable for full electron dynamics. Recently, the effect of ion drift instability in low-frequency mode is studied in a complex plasma considering weakly to the strongly collisional regions for different charged and neutral particles [58]

3.1 Motivation

Morzov [59] originally studied the $\mathbf{E} \times \mathbf{B}$ instability in plasma with inhomogeneous magnetic field and density gradients, and it was estimated that long wavelength modes dominate the anomalous transport of electrons. A density gradient tends to stabilize the instabilities for a collision-less, inhomogeneous, low β plasma with an external sheared magnetic field for a small magnetic shear limit when electron temperature is very high [60]. The central goal of this chapter is to propose an analytical model for $\mathbf{E} \times \mathbf{B}$ instability, developed for plasma with density gradient perpendicular to the sheared magnetic field considering constant collision frequency under the influence of an external sheared magnetic field. A three-dimensional fluid model for ions in an ionized plasma is used. The model differs from the existing ones through the approximation of constant collisional terms in the fluid equations and the influence of the externally applied sheared magnetic field.

This chapter introduces a differential equation presented in slab geometry and gives the eigenfunction and the dispersion relation derivations for the analysis of cross-field instability in the lower frequency region.

3.2 Formulation of the Problem

We introduce the influence of the shear magnetic field on an inhomogeneous plasma for constant collision frequency (ν) and try to find the stabilization criterion. The calculation is performed in slab geometry using a fluid model following the steps discussed in chapter 2.

We consider a collisional plasma under the influence of sheared magnetic field $\mathbf{B}=B_0 \left(\hat{z} + \frac{y}{L_s}\hat{x} \right)$, with an inhomogeneity in density profile of the form

$$n = n_0 e^{-i\omega t + \frac{y}{L_n}}$$

The density variation occurs along $\hat{y}$, where L_s and L_n are sheared length and the density gradient length respectively. We have undertaken a problem where we are studying the $\mathbf{E} \times \mathbf{B}$ flow under a non-uniform electric field and trying to solve the dispersion equation. The continuity equation, electron and ion momentum equation, and quasi-neutrality condition are used in this context.

$$\frac{\partial n_\alpha}{\partial t} + \vec{\nabla} \cdot (n_\alpha \vec{V}_\alpha) = 0 \tag{3.1}$$

Here, α denotes the charged species electron and ion respectively. In the presence of the collisions, we have to add the collision term ν in the equation of motion

$$M_\alpha \frac{d\vec{V}_\alpha}{dt} + M\nu \vec{V}_\alpha = q\left[\vec{E} + \frac{\vec{V}_\alpha \times \vec{B}}{c}\right] \tag{3.2}$$

Where, c, e, and M_α are the velocity of light, electron charge, and mass of the electron or ion respectively, $\vec{V}_\alpha$ represents the velocity ions. The components of the drift velocity of ions along the y-direction are calculated from the standard relation as follows,

$$v_x = \frac{-c}{B_0}\cos^2\theta \frac{\partial\phi}{\partial x}$$

$$v_y = \frac{-ikc}{B_0}\cos^2\theta$$

$$v_z = \frac{c}{B_0}\cos\theta\sin\theta$$

where, $Sin\theta = \frac{y/L_S}{\sqrt{1+(y/L_S)^2}}$ and $Cos\theta = \frac{1}{\sqrt{1+(y/L_S)^2}}$,

Here we assume the potential of the form $\phi(y,t) = \phi(y)e^{i(kx-\omega t)}$ the $\frac{\partial}{\partial z}$ term is absent as the shear occurs in a plane perpendicular to the magnetic field which is applied along the z direction. Equation (3.1) is the continuity equation for charge flow. And equation (3.2) is the ion momentum equation, where ν is the collision frequency, $\Omega_i = \frac{eB}{Mc}$ (ion cyclotron frequency) then replacing electric field,

$\vec{E} = -\vec{\nabla}\phi$. A relationship between n and potential can be derived from the continuity equation for electorns, which yields

$$\frac{\partial n}{\partial t} = -n\vec{\nabla}\cdot\vec{v} - \vec{v}\cdot\vec{\nabla}n \tag{3.3}$$

$$\frac{n}{n_0} = [\frac{-2kc}{L_s B_0 \omega} \cos^3\theta \sin\theta + \frac{kc}{L_n B_0 \omega} \cos^2\theta]\phi \tag{3.4}$$

Now, considering the ions are at equilibrium and using ion momentum relation, the parallel component of velocity ($V_\parallel$) and the perpendicular term of the velocity ($V_\perp$) can be expressed as,

$$V_\perp = \widehat{e_x} \left\{ -\frac{ke\varphi(\omega - kV + i\nu)}{M\Omega^2} \cos^2\theta - c\frac{\cos^2\theta}{B_0} \frac{\partial\phi}{\partial y} \right\}$$

$$+ \widehat{e_y} \left\{ \frac{ie(\omega - kV + i\nu)}{M\Omega^2} \frac{\partial\phi}{\partial y} + \frac{ik\varphi.c.\cos^2\theta}{B_0} \right\}$$

$$+ \widehat{e_z} \left\{ \frac{e\varphi.k(\omega - kV + i\nu)}{M\Omega^2} \sin\theta.\cos\theta + c.\frac{\sin\theta.\cos\theta}{B_0} \frac{\partial\phi}{\partial y} \right\}$$

with, n= n_0 + n′, $\vec{V} - \vec{v} = V_0$, here n′ and $\vec{v}$ are the perturbed number and velocity under the inhomogeneous electric potential. Here V_0 is the equilibrium velocity.

$$n_0\vec{\nabla}.(\vec{V} - \vec{v})] + (\vec{V} - \vec{v}).\vec{\nabla}n_0 + (\vec{V} - \vec{v}).\vec{\nabla}n' + n'\vec{\nabla}.(\vec{V} - \vec{v})] = 0 \tag{3.5}$$

$$(\boldsymbol{\nabla}_\parallel.V_\parallel) = \left(\frac{ik^2 \sin^2\theta}{(\omega - kV + i\nu)}\right) \frac{\partial}{\partial x} \frac{e\phi}{M}.$$

$$\boldsymbol{\nabla}_\perp(V_\perp - v_\perp) = \frac{-ik^2 e\phi (\omega - kV + i\nu)}{M\Omega^2} \cos^2\theta + \frac{ie(\omega - kV + i\nu)}{M\Omega^2} \frac{\partial^2\phi}{\partial y^2}$$

$$(V - v).\nabla n_0 = \frac{ie(\omega - kV + i\nu)}{M\Omega^2} \frac{1}{L_n} \frac{\partial\phi}{\partial y}.$$

$$\boldsymbol{V}.\nabla n' = ikVn.$$

Putting these values in equation (3.5)

$$kV \frac{n}{n_0} = -\left[\frac{e(\omega - kV + i\nu)}{M \Omega^2}\left\{\frac{\partial \phi^2}{\partial y^2} + \frac{1}{L_n}\frac{\partial \phi}{\partial y}\right\} + \frac{e\phi k^2 \sin^2\theta}{M(\omega - kV + i\nu)} - \frac{e\phi k^2 \cos^2\theta(\omega - kV + i\nu)}{M \Omega^2}\right] \qquad \textbf{(3.6)}$$

We simplify the above equation assuming, $\frac{\partial}{\partial x} = ik, \frac{\partial}{\partial z} = 0$ for shear and also neglect the $(\nu)^2$ where ν the collision frequency, Applying quasi-neutrality and comparing equations (3.4) and (3.6) we get the differential equation for the perturbed magnetic field the following second order differential equation is obtained,

$$\frac{d^2\phi}{dy^2} + \frac{1}{L_n}\frac{d\phi}{dy} - \left\{\frac{k^2\cos^2\theta}{(\omega - kV + i\nu)} - \frac{k^2\sin^2\theta\Omega^2}{(\omega - kV + i\nu)^2} - \frac{k^2\Omega^2 cMv\cos^2\theta}{B_0\omega e(\omega - kV + i\nu)}\left(\frac{2\cos\theta\sin\theta}{L_s} - \frac{1}{L_n}\right)\right\}\phi = 0 \quad \textbf{(3.7)}$$

finally, equation (3.7) is written as,

$$\frac{d^2\phi}{dy^2} + Q(y)\frac{d\phi}{dy} - R'(y)\phi = 0 \qquad \textbf{(3.8)}$$

Equation (3.8) describes the mode structure of ϕ for cross-field ($\mathbf{E} \times \mathbf{B}$) instability under the influence of an externally applied sheared magnetic field.

3.3 Derivation of the Dispersion relation

The dispersion relation is obtained as a solution of the set of model equations that describe the given waves, and it is written in the form D (k, ω) = 0. This establishes a relationship between wave vector (k) and the frequency (ω) of a wave that contains information about the direction of wave propagation and describes whether the wave can propagate or not under certain conditions. The roots of the dispersion equation correspond to the different modes of wave propagation. As the frequency is considered complex, the imaginary part of frequency (γ) describes the growth or damping rate of the wave, depending on the sign. For a given wave vector, usually,

more than one solution of a complex frequency can exist. The dispersion relation depends on the effective magnetic and electric field in plasma, phase space distribution functions, the properties of a plasma, and properties of the particles i.e. mass and charge of different particles in plasma.

3.3.1 Local Analysis

The local theory of dissipative drift wave is applicable for shear-less conditions as the inclusion of shear strongly modifies the results. At this local approximation, one can get the general solution for the $\mathbf{E} \times \mathbf{B}$ instability and maximum growth rate in the plasma with a density gradient. We first reduce the differential equation to an algebraic equation by making use of Fourier transform to get the general dispersion relation. Here we take, $\dfrac{\partial}{\partial y} \rightarrow ik_y,$

$L_s \rightarrow \infty$, i.e. $\theta \sim 0$. In the zero magnetic shear and small wave number limit the density gradient is stabilized and the eigenfunction is uniform in the space [61]. In this limit, the differential equation (3.8) reduces to the following algebraic equation

$$k_y^2 + i\frac{k_y}{L_n} = \frac{k^2\left(1+\frac{\Omega^2 cMV}{L_n B_0 \omega e}\right)}{(\omega - kV + i\nu)} \tag{3.9}$$

3.3.2 Nonlocal Analysis

So far, the local approximation of the differential equation has been taken into consideration for the limiting case of infinite magnetic shear length. In this chapter we have undertaken a problem where the cross-field instability is studied under a non-uniform electric field and the shear is also a function of y, so we cannot apply Fourier

transform generally which is along the y direction. In order to solve the equation

(3.10) we reduce the equation by considering $\frac{d^2\phi}{dy^2} = \phi''$ and $\frac{d\phi}{dy} = \phi'$ in the form,

$$\phi'' + Q(y)\phi' + R(y)\phi = 0.$$

where $Q(y)$ and $R(y)$ are the coefficients of ϕ' and ϕ respectively in (3.9).

$$R(y) = -R'(y)$$

$$= -\left\{ \frac{k^2\cos^2\theta}{(\omega - kV + i\nu)} - \frac{k^2\sin^2\theta\Omega^2}{(\omega - kV + i\nu)^2} \right.$$

$$\left. - \frac{k^2\Omega^2 cMv\cos^2\theta}{B_0\omega e(\omega - kV + i\nu)} \left(\frac{2\cos\theta\sin\theta}{L_s} - \frac{1}{L_n} \right) \right\}$$

$$\eta = \frac{cVM\Omega}{e\omega B_0} \text{ , } p = \frac{\Omega}{(\omega - kV + i\nu)}$$

$$R(y) = -\left\{ \frac{k^2}{\left[1 + \left(\frac{y}{L_s}\right)^2\right]} - \frac{k^2 p^2 (y/L_s)^2}{1 + \left(\frac{y}{L_s}\right)^2} - k^2\eta p \left[\frac{2\left(\frac{y}{L_s}\right)}{\left[1 + \left(\frac{y}{L_s}\right)^2\right]^2 L_s} - \frac{1}{L_n\left[1 + \left(\frac{y}{L_s}\right)^2\right]} \right] \right\} \qquad \textbf{(3.10)}$$

In the zero magnetic shears, i.e. $L_s \to \infty$ the above differential takes a simplified form,

taking the real part only (for small wave number approximation)

$$\frac{d^2\phi}{dy^2} + \frac{1}{L_n}\frac{d\phi}{dy} - k^2 \left\{ \frac{k^2\Omega^2 cMV}{B_0 e(\omega - kV)^2 + \nu^2)} \left(\frac{1}{L_n} \right) \right\} \phi = 0 \qquad \textbf{(3.11)}$$

for finite shear (3.12) can be expanded as,

$$R(y) = a_0 + a_1 y + a_2 y^2 + a_3 y^3 + a_4 y^4 + \ldots.. \qquad \textbf{(3.12)}$$

collecting the coefficient of different power of y and comparing it with the

equation (3.10), we keep up to the term y^2,

29

$$a_0 = -k^2 + \frac{k^2 \eta p}{L_n}$$

$$a_1 = \frac{-2k^2 \eta p}{L_s}\left(\frac{1}{L_s}\right)$$

(3.13)

$$a_2 = \left[\frac{-k^2}{L_s{}^2} - \frac{2k^2 p^2}{L_s{}^2} + \frac{k^2 \eta p}{L_n L_s{}^2}\right]$$

where, $\eta = \frac{cVM\Omega^2}{e\omega}$, $p = \frac{\Omega}{(\omega - kV + i\nu)}$

to make further analytic calculations we define a new coordinate system,

$$\xi' = (-a_2)^{\frac{1}{4}}\left(y + \frac{a_1}{2a_2}\right)$$

(3.14)

$$y = \xi'(-a_2)^{-\frac{1}{4}} - \frac{a_1}{2a_2}$$

(3.15)

Following the methodology described in ref. [62] equation (3.11) reduced to Weber's equation

$$\frac{d^2\phi}{d\xi'^2} + (-a_2)^{-1/4}\rho_s'\frac{d\phi}{d\xi'} + (E' - \xi'^2)\phi = 0$$

(3.16)

where, $\quad E' = \frac{\left(a_0 - \frac{a_1{}^2}{4\,a_2}\right)}{(-a_2)^{1/2}}$

now define a new potential

$$\phi = \phi_k \exp(1/2)[-\int \beta * d\xi']$$

(3.17)

where, $\beta = \frac{1}{2}(-a_2)^{-1/4}\rho_s'$

the second term in the equation (3.11) will be removed and get the following radial eigenvalue equation,

$$\frac{d^2 \phi_k}{d\xi'^2} + (E^* - \xi'^2)\phi_k = 0 \tag{3.18}$$

where $E^* = E' - \left[\frac{1}{2}(-a_2)^{-\frac{1}{4}}\rho'_s\right]^2$

using the standard solution procedure for the above equation we can write,

$$\Phi_{kl} = \Phi_0 \exp\left[-\frac{\xi'^2}{2}\right] H_l(\xi')$$

with, $E^* = 2l+1, \; l = 0, 1, 2, 3\ldots\ldots$

Here $H_l(\xi')$ is the lth order Hermite polynomial. Being the most dominant we consider the lowest order mode $l = 0$ for which the solution of the equation (3.18) gives the eigen function, $\Phi_k = \Phi_0 \exp(-\frac{\xi'^2}{2})\exp(-\beta.\xi')$.

Putting the value of β and ξ', the corresponding eigenfunction equation (3.18) takes the form,

$$\Phi_k = \Phi_0 \exp\left[-\frac{1}{2}i(a_2)^{\frac{1}{2}}\left(y + \frac{a_1}{2a_2}\right)^2\right]\exp\left[-\frac{1}{2}\rho'_s\left(y + \frac{a_1}{2a_2}\right)\right]$$

By rearranging the variables, the above expression of potential can be rewritten as,

$$\Phi_k = \Phi_0 \exp\left[-\frac{1}{2}i(a_2)^{\frac{1}{2}}\left(y + \frac{a_1}{2a_2} + \frac{\rho'_s}{2\sqrt{-a_2}}\right)^2\right].\exp\left[\frac{i\sqrt{a_2}}{2}\left(\frac{\rho'_s}{2\sqrt{-a_2}}\right)^2\right] \tag{3.19}$$

Here we can see the eigen function is shifted off and it depends on the factor$(-\frac{\rho'_s}{2\sqrt{-A_2}})$. Now separating the above function into real and imaginary parts by assuming,

$\sqrt{a_2} = p' + iq'$, and $\frac{a_1}{2a_2} = \alpha' + i\beta'$

Separating in the to real part and imaginary part the above equation takes the form,

$$\Phi_k = \Phi_0' \exp\left[\frac{-q'}{2}\left\{y + \left(\alpha' + \frac{\beta'p'}{q'} - \frac{\rho_s'}{2q'}\right)\right\}^2\right] \times \exp\left[\frac{ip'}{2}\left(y + \alpha' - \frac{\beta'q'}{p'}\right)^2\right] \qquad \textbf{(3.20)}$$

The real part can be expressed as a standard form and the equation gives,

$$\Phi_k = \Phi_0' \exp\left[\frac{-1}{2}\left\{\frac{y-\sigma}{\delta}\right\}^2\right] \times \exp\left[\frac{-ip'}{2}\left(y + \alpha' - \frac{\beta'q'}{p'}\right)^2\right] \qquad \textbf{(3.21)}$$

where, $\sigma = -[\alpha' + \frac{\beta'p'}{q'} - \frac{\rho_s'}{2q'}]$ is the mode shift, and the mode width can be written

as, $\delta^{-2} = -q'$ that is, the imaginary part of the a_2. It is clear that to separate the

equation (3.21) into real and imaginary the balancing terms are

absorbed in the amplitude part Φ_0' of equation (3.21) which satisfies the physical

boundary condition as $y \to \pm\infty$, $\varphi \to 0$. So the mode decays with y and does not

propagate, so this gives that, the eigenmode localized about the mode rotational

surface.

$$\Phi_{Re} = \Phi_0' \exp\left[\frac{-1}{2}\left\{\frac{y-\sigma}{\delta}\right\}^2\right] \times \cos\left[\frac{p'}{2}\left(y + \alpha' - \frac{\beta'q'}{p'}\right)^2\right]$$

$$\Phi_{Im} = -\Phi_0' \exp\left[\frac{-1}{2}\left\{\frac{y-\sigma}{\delta}\right\}^2\right] \times \sin\left[\frac{ip'}{2}\left(y + \alpha' - \frac{\beta'q'}{p'}\right)^2\right]$$
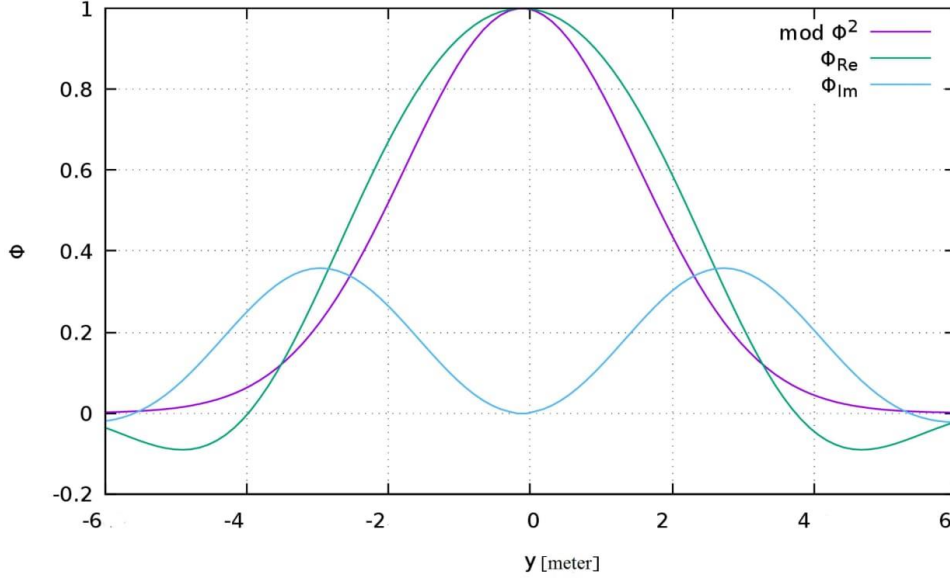
Fig 3.1: Variation of normalized wave function with y.

3.4 Eigenvalue calculation

Now, the eigenvalues are obtained by solving the following eigenvalue equation which gives the dispersion relation for finite shear,

$$1 = \frac{\left(a_0 - \frac{a_1^2}{4\,a_2}\right)}{(-A_2)^{\frac{1}{2}}} - \left(\frac{1}{2}(-a_2)^{-\frac{1}{4}}\rho_s'\right)^2$$

$$4\left(\frac{k^2\eta p}{L_n} - k^2\right) - \frac{\left(\frac{2k^2\eta p}{L_s^2}\right)^2}{\frac{k^2}{L_s^2}\left(1 + p^2 + \frac{\eta p}{L_n}\right)} - \frac{1}{L_n^2} = 4i\left[\frac{k^2}{L_s^2}\left(1 + p^2 + \frac{\eta p}{L_n}\right)\right]^{\frac{1}{2}}$$

Here we assume $\eta \gg 1$ And Let, $\frac{L_n}{L_s} = s$

$$k\eta p\left[s + \frac{1}{s}\right] - \frac{1}{4ks} = -\left(\frac{\eta p}{L_n}\right)^{\frac{1}{2}}$$

Squaring both sides and rearranging the terms,

33

$$k^2\left(s+\frac{1}{s}\right)^2(\eta p)^2 - \eta p\left(\frac{1}{2}+\frac{1}{2s^2}-\frac{1}{L_n}\right) = -\frac{1}{4ks}$$

$$\text{let,}\quad \eta = \frac{cVM\Omega^2}{e\omega} = \frac{\eta_1}{\omega}\,;\qquad p = \frac{\Omega}{(\omega-kV+i\nu_{ie})}\,;$$

$$\left(s+\frac{1}{s}\right)^2 = s_1;\quad \left(\frac{1}{2}+\frac{1}{2s^2}-\frac{1}{L_n}\right) = D$$

$$\frac{s_1(k\eta_1)^2}{\omega}\left(\frac{\Omega}{(\omega-kV+i\nu)}\right)^2 - \frac{D\eta_1}{\omega}\left(\frac{\Omega}{(\omega-kV+i\nu)}\right) = -\left(\frac{1}{4ksL_n}\right)^2 \qquad\text{(3.22)}$$

Rearranging the above equation we get the dispersion relation,

$$\omega^4 + 2\omega^3(i\nu - k\mathrm{v}) + \omega^2[(k\mathrm{v})^2 - \nu^2 - 2i\nu k\mathrm{v} - D\eta_1\Omega] + \omega[D\eta_1\Omega(kV - i\nu)]$$

$$+ 16k^4\eta_1^2(\Omega sL_n)^2 s_1 = 0$$

Solving the above dispersion relation is using **MATLAB** root finding root-finding routine I get the real wave frequency ω_r and growth rate γ. The dispersion relation of the two branches have equal roots with real wave frequency ω_r and growth rate (γ) with same absolute value but with opposite sign. For further graphical analysis we used the, values of **Table: 1**.
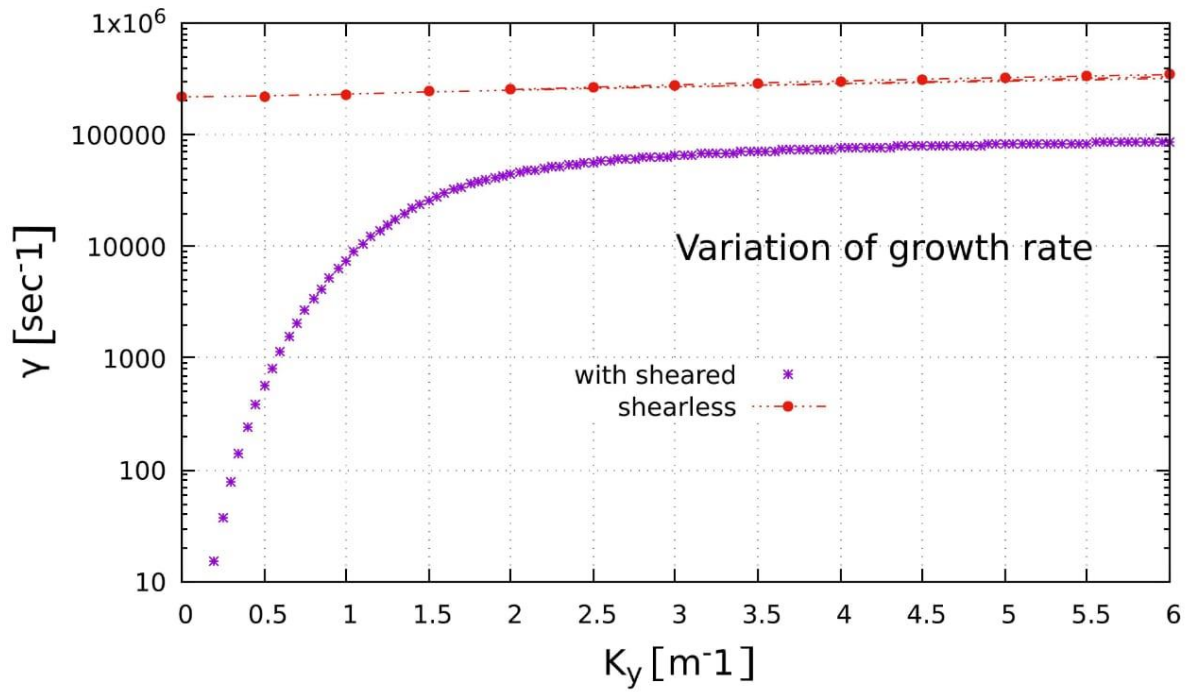
Fig 3.2: Variation of growth-rate with wavenumber, k_y.
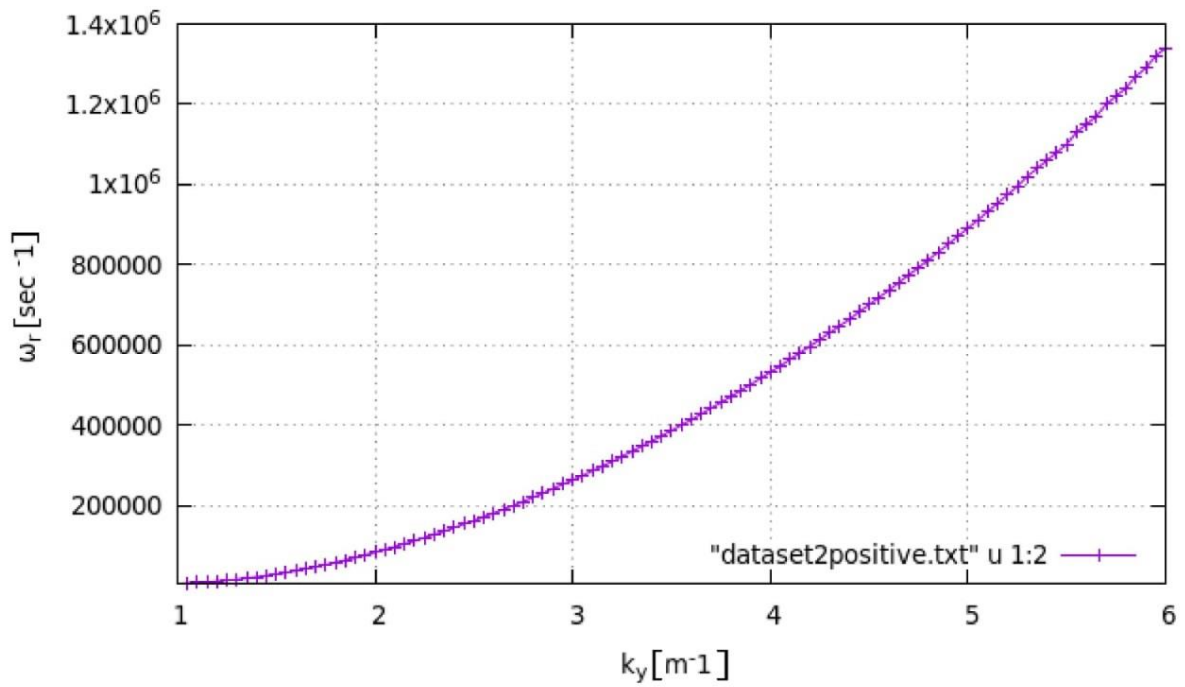
Fig 3.3: Variation of real part of frequency with wavenumber, k_y.

Table: 1

Parameters used for stability analysis [63]

Name of the variables	Values with unit
R(major radius)	75 cm
B_T (toroidal magnetic field)	1.2 tesla
n_e (electron number density)()	$3.8 \times 10^{19}\,\text{m}^{-3}$
T_i (ion temperature)	150 eV
q (quality factor)	3
s (Shear)	1
Shear length	2.25 m
R(major radius)	0.015 m
Collision frequency	$2.194 \times 10^5\,\text{s}^{-1}$
M (ion mass)	1 amu

Collision frequency (ν), ion gyro frequency (Ω) used in this analysis are calculated using standard relations.

3.5 Result and discussion

Initially, the observation of the drift instability was based on a local analysis in a shearless slab geometry in which the wavenumber parallel to the ambient constant magnetic field. A methodology was later developed for nonlocal analysis [20], [21] in sheared slab geometry and a criterion was found for suppressing the instability by magnetic shear. The characteristics of the wave modes are understood as an outcome of perturbations from the unstable region toward the stable surroundings. The eigenmode equation in wave-number space usually describes the nonlocal behavior of these waves, where local instability criteria are not satisfied.

A theoretical analysis has been done here in slab geometry for externally applied sheared magnetic field, focusing on ion drift waves in the small wave number region $[k\rho_i < 1]$ where ρ_i is the ion Larmor radius. This calculation gives eigen function φ and eigenvalue, considering the density scale length (L_n) and sheared scale length (L_s) in a resistive plasma. General normalized behaviour of eigen modes with its real and imaginary part illustrated in fig-3.1 at the stabilized region of the growth rate curve. The localization of mode structure about the rational surface is obtained. There a mode shift occurs is a function of $(-\frac{\rho'_s}{2\sqrt{-A_2}})$ due to the presence of magnetic shear. The wave packet localizes around the long wave length region. As the flow localized at the resonant radius, a large shear flow is expected [64].

Nonlocal analysis may predict multiple unstable modes existing in this region, this is especially observed for the long wavelength modes which offer a larger

contribution to the anomalous transport [65]. The imaginary part of the solution gives the condition of stabilization. In fig-3.2 we plot the growth rate variation concerning wave number. The nonlocal growth rate turned out to be smaller compared to the shear-less growth rate. This implies that the magnetic shear reduces the growth rate [66]. Here, we observe that the $\mathbf{E} \times \mathbf{B}$ instability is stabilized more by the magnetic shear at a smaller wave number. If we compare, fig-3.2 and fig- 3.3 it shows that growth rate (γ) tends to attain the magnitude of real frequency (ω_r) after a certain range while the variation with a concerning number is studied. The perturbed density profile provides a destabilizing effect in the form of inverse Landau damping for magnetic shear-driven resistive drift mode [67]. This implies that the solution describes a propagating wave and the mode becomes unstable in that region. The influence of destabilizing effect on an equilibrium by current parallel to magnetic field on drift waves in a collisional, sheared slab plasma is that the current levels needed to overcome the dissipative damping [53]. Additionally, we found that collision frequency being relatively small does not significantly affect the ion drift eigenmode.

3.6 Future Work Plan

Drift instabilities are related to plasma polarization caused by magnetic drift of the charged particles. These instabilities will lead to different impacts of magnetic shear on ions and electrons. It was found experimentally that at large values of applied electric fields, the main cross-field modes give rise to several modes possibly through nonlinear wave-wave interactions, which play an important role in the saturation of

cross-field instability [51]. Also, the complete experimental description of drift instability is mostly impossible, either because of very high temperatures of fusion-grade plasmas or due to the configuration restrictions on confinement devices [68]. I shall extend this work to the toroidal eigenfrequency, and eigenfunction calculation considering the pressure gradient effect to implement an improved model for studying the collisional effect on dispersion relation and growth rate. I can also calculate the associated quasilinear transport coefficients eigenmode for different shear length values of magnetic field. So it is expected that in toroidal geometry for finite β, the properties mentioned above show little difference compared to the slab model at very low β in the electrostatic limit. This will lead to little more realistic theoretical predictions of the electromagnetic eigenfrequency, eigenfunction for stability analysis.

Chapter 4

Effect of Two Different Electrons Temperatures in Auroral Ionosphere

One of the Earth's atmosphere's most interesting sights is the auroral zone. A wide variety of plasma physics events, such as large-scale MHD phenomena, radio emissions, solitary waves, and microphysics of plasma instabilities, take place on auroral field lines. The formation of the aurora depends on the field-aligned acceleration of electrons, which is caused by the field-aligned potential drop associated with FACs (field aligned current), which results in the field-aligned acceleration of electrons necessary for the aurora's production. We will briefly review some of the fundamental ideas related to the Ionosphere in this chapter before getting into the specifics of our topic, which involves examining the impacts of two different electron temperatures in the presence of ions in an auroral Ionosphere.

4.1 Ionosphere

The Ionosphere is an atmospheric layer consisting of partially ionized gasses (plasma) mainly caused by solar extreme ultraviolet (EUV) photo-ionization during daylight and X-ray, as well as by impact ionization through energetic particle precipitation. Photo-ionization is the Ionosphere's primary source of plasma production in ionosphere [69]. Several other processes affect the plasma densities in the ionosphere occur, like recombining ions with electrons, transport or diffusion of ions and chemical reactions between ions and neutrals [70]. Electric currents in the atmosphere

were the reason for variations in the magnetic field. It plays an important role in the propagation of radio waves. It causes signal scintillation and modification of the earth's current system, both on the ground and in the upper atmosphere. Thus, this layer affects communication systems and navigation. The ionosphere typically starts around 60 km altitude, continues through the thermosphere, and ends at about 1500 km in the exosphere (Fig. 4.1). However, the boundary layer is not sharp and it varies with the presence of free thermal (< 1 eV) electrons and ions. The Ionosphere is divided into different regions with the following roughly defined range, D-region below 90 km, E-region from 90 km to 150 km, and F-region above 150 km (Fig.4.3). In addition, in daylight, the F-region is divided into F1 and F2 layers, below and above the maximum plasma density height, respectively.
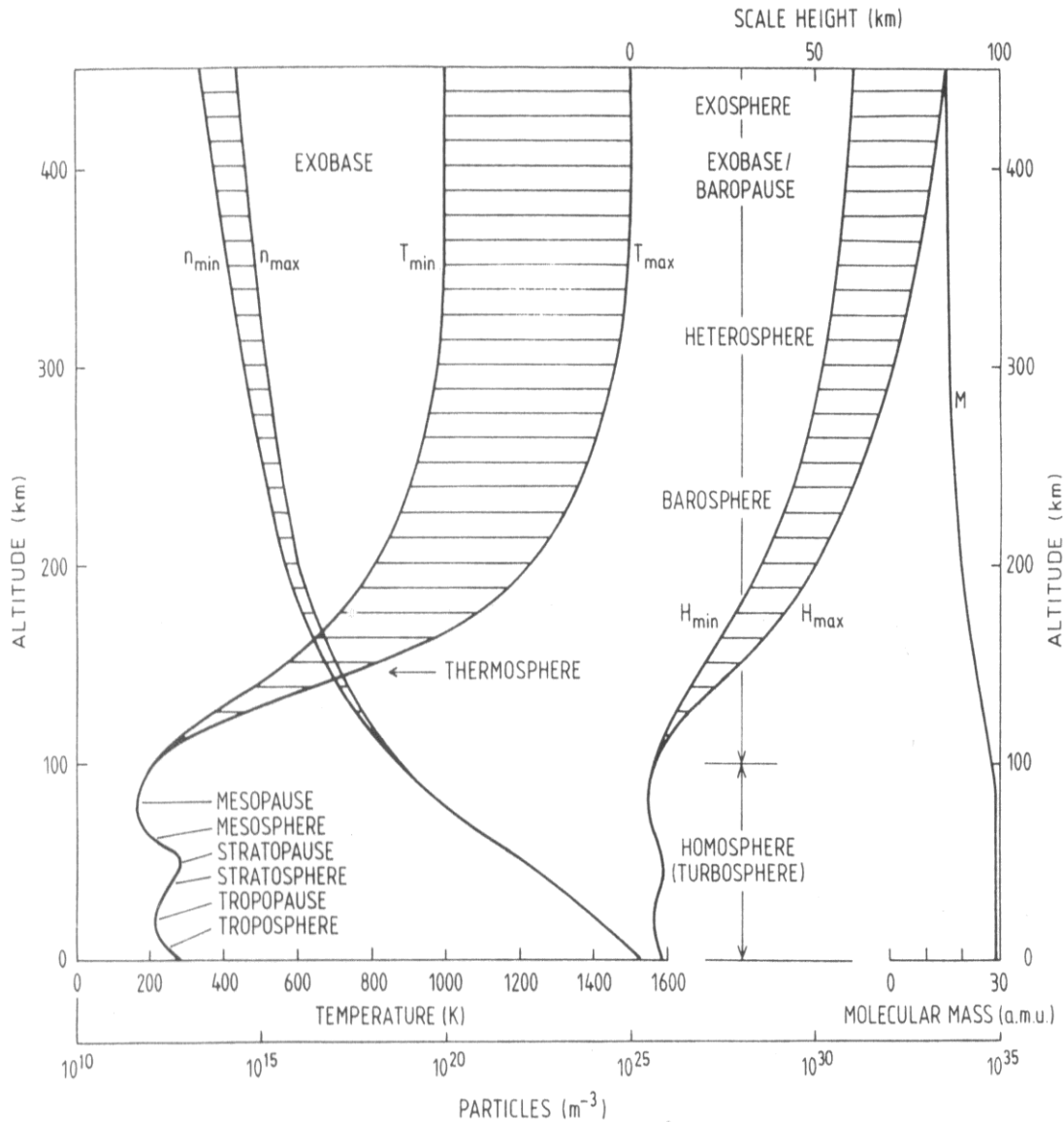
Fig. 4.1: Model height profiles of temperature T, density n, molecular mass M, and scale height H in the lower 450 km of the Earth's atmosphere [69] *in response to solar activity.*

A third sub-region, known as the upper F-region (> 600 km), also exists above the F2 peak. In the high F-region, where the neutral density is very low, the action of the Sun's ionization radiation produces very few electrons. The ionization of atmospheric

gases, specifically N2, O2, and ionized O, results in the formation of the ionosphere. The reflection of a radio wave, depends on the critical plasma frequency in the ionosphere. This frequency is the highest frequency to be reflected from the ionosphere, and it happens when the radio frequency is equal to the plasma frequency and is given by,

$$f_c = 9\sqrt{N}$$

The ionosphere represents less than 0.1% of the total mass of the Earth's atmosphere. At sea level, the atmospheric density is about $1.3 \, kg/\, m^3$, while at 300 km, it is reduced to only $10^{-12} \, kg/\, m^3$ ($10^{-11} \, kg/\, m^3$) during average solar flux. The number density of all species of the atmosphere decreases monotonically with a height from $10^{25} \, /m^3$ to $10^{15} \, /m^3$ at ground level and $10^{10}/m^3$ at 1000 km [69].

The ratio of charged particles to neutral particles concentration varies between 10^{-8} at 100 km and 10 N at 1000 km during the daytime, whereas at the typical height (~300 km), the plasma density is maximum, the ratio is 1 electron per 10 thousand neutrals (i.e. 10^{-4}). The electron density varies with height and depends on the time of day, season, sun-spot number and degree of the disturbed Ionosphere. Typical electron densities at high latitudes during day and night are less than 10^{10} to 10^{12} m^3 respectively. In the F-region (Fig. 4.2) the Absence of sunlight generally causes less density. However, despite a smaller solar zenith angle in summer, the electron density is higher during winter than in summer, above and around 200 km. The seasonal anomaly occurs because of seasonal changes in the neutral atmosphere. The O/N_2

ratio increases and decreases in the winter and summer hemispheres respectively,

resulting in a higher O density in the F-region altitudes during wintertime [69].
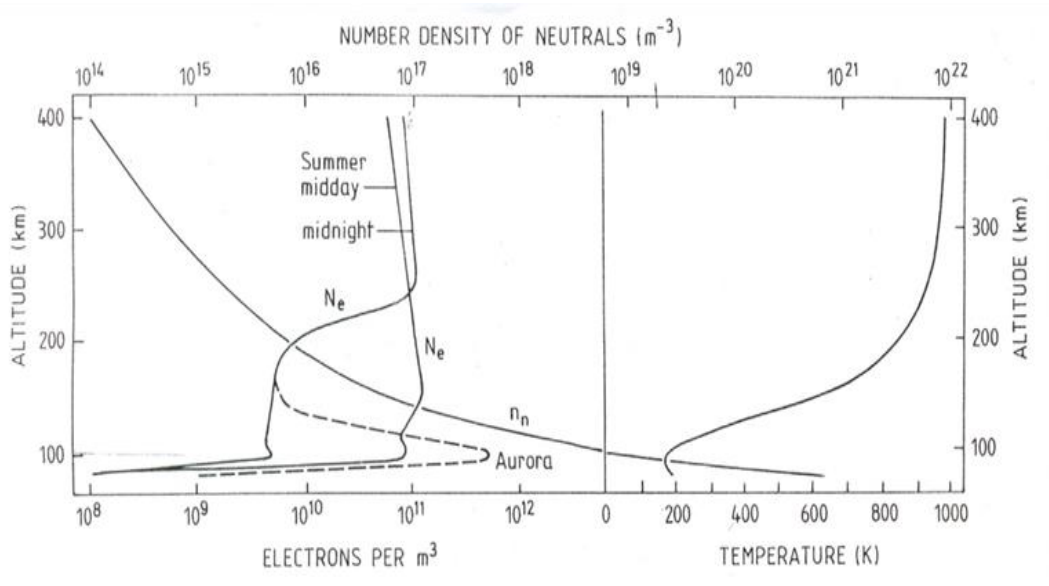

Fig. 4.2. An electron density profile represents the average daytime and night-time conditions at high latitudes. (The dashed line indicates the density profile for auroral conditions. The background neutral density profile also with an average neutral atmosphere temperature profile is schematically illustrated. [69])
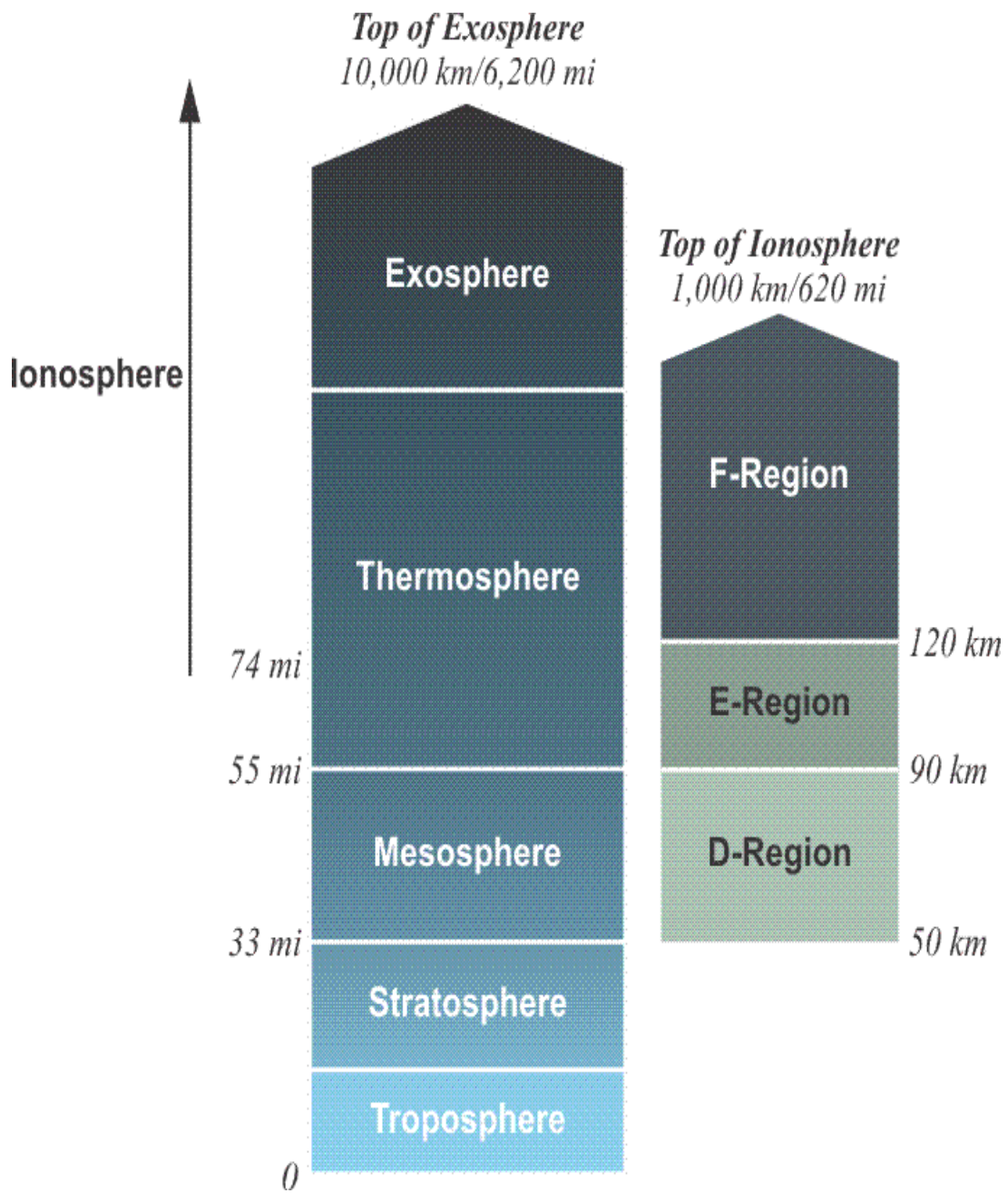
*fig: 4.*3 Atmospheric Model [71]

4.2 Aurora

The aurora represents the visible manifestation of a chain of interactions between solar wind, the ionosphere and the magnetosphere. The energy gained from slowing down the solar wind as it encounters the Earth's magnetosphere is transformed into field aligned guided fluxes of charged particles, producing aurora. Auroral emission results from the excitation of atmospheric atoms and molecules by the impinging charged particles. Almost all auroral light consists of emission lines and bands of ionized O, N or neutral O_2, N_2 [72]. Visual aurora can have different forms, such as arcs, folds, spirals, curls, etc. Their sizes range from several hundred meters to several hundred kilometers, all the way up to the size of the entire auroral oval. At night time, about 120 km the aurora density could reach around 10^{-12} m^{-3} within a few tens of seconds. At this time both the pressure and collision frequency decrease with height. Also with the increased neutral density, the collision frequency increases between ionized species and neutrals. In the upper F-region, the collision frequency decreases with the neutral density. At higher altitudes, diffusion is crucial. Ions and electrons respond to these collision frequencies in different ways. In light of the ionospheric electric currents below 120 km, they, therefore, therefore play a significant role in ionised plasma. Above about 180 km, the plasma is fully ionized, and the collision frequencies of charged particles becomes much higher so the charged particles can ignore the neutrals [70].

The magnetic field, in general, controls charged particles. However, the circular motion in a uniform magnetic field does not change the particle's kinetic energy. If the ion collision frequency is larger than the ion gyro-frequency, the ions are not

magnetized, and at the same time, the electrons are magnetized. Electron interactions with the thermosphere lead to the ionisation and excitation of thermospheric oxygen and nitrogen, which ultimately results in the formation of auroral emissions and ionisation that can be seen. This enhances the background electron number density and ionospheric conductivity. A wide variety of transport and chemical processes affect the distribution of ionospheric plasma in auroral current systems. In a typical auroral system, the field aligned currents are carried by electrons, while the current is closed by ion motions perpendicular to the geomagnetic field through the E-region [73].

4.3 Role of Collision Frequency in Ionosphere

The collisional phenomena are very important in space plasmas and fusion plasmas [74]. The Earth's ionosphere below the F-region is not fully ionized, since the number of neutral collisions with ions and electrons is considerable in both the E- and D-regions. The collision frequency is thus comparable to or larger than the plasma frequency. However, above 200 km, the ionospheric plasma can be considered as fully ionized because plasma frequency is much larger than the electron and ion collision frequencies. The charged particles do not interact with neutrals, except in a few occurrences where the ion-neutral collisions are important, such as Joule heating in the F-region. However, if the charged particles frequently collide with neutrals, the electrons will be forced into equilibrium and the medium becomes a neutral gas, not Plasma anymore! and this happens at night when there is no ionization source (no UV radiation, except for energetic particles at high latitudes). For an ionized medium the basic criterions for the presence of Plasma in any medium are, i) the physical

dimension of the system must be large compared to the Debye length, ii) the plasma inside a Debye sphere must contain number of particles, and iii) the electron to be remain unaffected by collisions with the neutrals. Electron-neutral collision frequency must be much smaller than the plasma frequency ($\upsilon_{en} \ll \upsilon_{pe}$). The gyro frequency is also important as it determines the ion and electron dynamics in the E-region. If the ion neutral collision frequency is larger than the ion gyro frequency ($\upsilon_{in} \gg \Omega_e$,) the ions are not magnetized. At the same time, the electrons are magnetized as the electron collision frequency is less than the electron gyro frequency ($\upsilon_{en} \ll \Omega_e$), and this could cause an enhanced electric current in the E-region. In the F- region, the collision frequency is always less than the gyro frequency ($\upsilon \ll \Omega_e$) while in the D-region, the collision frequency is always greater than the gyro frequency ($\upsilon \gg \Omega_e$). Charged particles that are not magnetized in the D-region will follow the neutral wind with the same velocity, while in the F-region, the charged particles will follow the cross-field drift ($\mathbf{E} \times \mathbf{B}$). So only the neutral wind component along the magnetic field line may affect the plasma drift.

4.4 Temperature

In the Ionosphere, the temperature (thermal energy) of a particle is directly proportional to average random kinetic (translational) energy. The neutral temperature will, in general, increases dramatically above the mesopause (~80km) into the thermosphere until it reaches an overall maximum of about 1000K. However, the maximum and minimum of the neutral temperature depend on time, latitude, solar activity and luminance. The temperature usually fluctuates between midnight and noon during solar minimum (maximum) from 1000K - 1700K [69]. In the ionosphere,

different temperatures of electrons, ions and neutrals can exist. During geomagnetic quiet conditions at altitudes larger than 110 km., the relation between the electron temperature (T_e), the ion temperature (T_i) and the neutral temperature (T_n) is : $T_e \geq T_i \geq T_n$. The mass difference between an electron and a neutral is huge. Hence, it is much easier for electrons to depart from the thermal equilibrium with decreasing electron neutral collision frequency than correspondingly for ions. The electrons are heated by photo-electrons created by UV solar radiation, while electrons heat up ions. Since the electron heating rate is larger than the electron to ion heat transfer, this causes $T_e > T_i$. The electron heat conduction determines how much T_e will be larger than T_i. However, during disturbed geomagnetic conditions, the ion temperature can get higher than the electron temperature at about 120 km due to heating caused by a strong electric current (≥ 106 A). Above 150 km altitude, the electron temperature is twice the ion temperature $T_e \approx 2T_i$, and the ion and electron temperature increase from (650–1500)K and (1300 – 3500)K, respectively, until it reaches the topside ionosphere. At lower altitudes, below 110 km, the electron, ion, and neutral temperatures are forced into a state of thermal equilibrium ($T_e \approx T_i \approx T_n$) by a very high collision frequency between charged and neutral particles. Ion-neutral collisions are elastic, while electron-neutral and electron-ion (Coulomb) collisions are inelastic. The energy, mass and momentum of the colliding particles are conserved in this collision process. Ion-neutral collisions are usually elastic because ions have thermal energy, which is inadequate to excite internal degrees of freedom. On the other hand, electron-neutral collisions can be inelastic when the electrons are photo-electrons with enough energy to excite internal degrees of freedom, such as ionization,

chemical reactions and electron excitation. Also, rotational, vibrational and fine structure excitations have a cooling effect on the thermal electron population. But the primary route for energy loss is the Coulomb collisions with the adjacent ions. At high latitudes, the electron heating caused by Joule heating and the particle heating caused by energetic charged particles are of great significance. The particle heating rate is found to be roughly 30% of the particle energy flux [75], and it is proportional to the electron density square, while The joule heating rate are estimated along the latitudinal extent of the auroral oval on the basis of magnetometer data and from Chatanika radar data [76]. Joule heating occurs mostly in the auroral region and is typically stronger at dawn than dusk.

4.5 Instability in Ionospheric Plasma

When the plasma is not in thermal equilibrium, instability occurs under certain conditions. If thermal fluctuations of plasma grow exponentially, the plasma becomes unstable. Such plasma instabilities occur if waves' intensity/ amplitude grow far from thermal equilibrium. Due to thermal fluctuations, the Langmuir and Ion-Acoustic waves are fundamental waves that always exist in plasma. Plasma waves can grow if the plasma is sufficiently anisotropic, which modifies the distribution through wave-particle interaction. Also, when the relative drift velocity between electrons and ions exceeds the local Ion-Acoustic speed, the system is unstable and excited electrostatic plasma waves heat electrons. Particle acceleration (as in aurora), wave-particle interaction and wave-wave interaction are all examples that can lead to instability processes that occur regularly in a plasma. Ionospheric instabilities are exhibited at all latitudes, longitudes and almost all altitudes. These irregularities are generally

50

magnetic field aligned, i.e. there are hardly any variations along the geomagnetic field. These are exhibited with scale sizes ranging from many kilometers to tens of centimeters during equatorial spread F. In geo-space, the most familiar instabilities are the two-stream instability (Farley-Buneman), one is the gradient drift instability (Rayleigh-Taylor) and the other is Kelvin-Helmholtz instability. If a stream of electrons and ions differ in velocity by more than the ion-acoustic speed, this two-stream instability produces electrostatic waves that propagate perpendicular to the magnetic field. Such instability occurs in the electro-jets in the E-region. The gradient-drift instability is also known as $\mathbf{E} \times \mathbf{B}$ drift instability. As long as the collision frequency is smaller than the gyro-frequency, the negative electrons and positive ions move in opposite directions when a force acts at right angles to a magnetic field. If the plasma density in the edge away from the force increases, gradient-drift instability may occur. The effective force is gravity, which may discontinue irregular structures in the F-region and produce structures in injected ion clouds. A typical product of a Kelvin- Helmholtz instability would be the shear Alfvén waves and generation of certain magnetic pulsations in the magnetosphere. It also tends to produce vortices, and the instability often occurs at the interface between two media in relative motion, which depends on the presence of a velocity shear. The electron-acoustic instability for $T_i > T_e$ may occur in some present-day Ө-pinches and mirror machines

4.6 Plasma Waves

In general, there are three main types of waves in plasma: i) Electrostatic waves ii) Electromagnetic waves and iii) Low-Frequency magnetized Plasma waves (e.g. Alfvén). The low-frequency magnetized plasma waves must consider both the ion

and electron motions. Electrostatic waves are divided into a high-frequency electrostatic plasma wave (the Langmuir wave) and a low-frequency electrostatic plasma wave (the Ion-Acoustic wave). These two waves do not have a wave magnetic field. The latter can only propagate through unmagnetized plasma if the frequencies are higher than the plasma frequency. In general, in a wave motion, the energy oscillates in different ways. For example, in a Langmuir Wave, the energy exchange is between kinetic particles and electric field energies. In Ion-Acoustic waves, the energy exchange is between kinetic and potential energies; in Alfvén Waves, the energy exchange is between kinetic and magnetic field energies. Whenever plasma is disturbed, the electron will start to oscillate with a certain plasma frequency. This oscillation will later on decay due to the damping effect from collisions. A spatially localized perturbation in cold plasma will not propagate at all but will oscillate at the plasma frequency, but if the pressure is included like in warm plasma, this will result in a propagating wave, known as an Electron plasma wave or Langmuir wave [MHz]. Electrons in thermal motion carry information into surrounding regions about what is going on in the oscillating region. Thus, the Langmuir wave has a frequency close to the resonance frequency of the cold plasma, of which the particles are initially at rest, with no random thermal velocities. In the framework of the incoherent scattering of radio waves, the width of the plasma lines depends on the damping of the Langmuir wave. Their frequency increases with increasing electron density. The ions are too heavy to respond, so only the electrons contribute to the Langmuir wave. As long as the collision frequency is less than the gyro frequency, the negative electrons and

52

positive ions move in opposite directions when a force acts perpendicular to a magnetic field. If the plasma density increases at the edge away from the force, gradient drift instability can occur. On the other hand, the ions play an important role in ion acoustic waves [kHz] because they control the electrons, although they are not involved in radar backscatter. This wave is analogous to sound waves in neutral gas in that they both propagate longitudinally, but an important difference is that the ion acoustic wave involves electrostatic forces. Thus, this wave occurs over a wide range of wavelengths and propagates in any direction in unmagnetized plasma and along the magnetic field in magnetized plasma (the same propagations apply to a Langmuir wave). The amplitudes of the electron and ion oscillations are not quite the same, and the resulting Coulomb force provides the potential energy to drive the waves. The Ion-Acoustic frequency is proportional $\sqrt{\frac{T_i}{m_i}}$, T_i is ion temperature and m_i the ion mass, and since the ion temperature increases with height, so does the ion acoustic frequency. This is also the case if a thermal motion occurs. If the wave gains more energy from electrons than it loses to electrons, the Ion-Acoustic wave will grow. If the temperature ratio between electrons and ions in plasma varies, different behavior cases may arise such as, i) $T_e/T_i \approx 1$, the Landau damping is strong as the phase velocity of the Ion-Acoustic mode is comparable to the ion thermal speed, ii) $T_e/T_i = 2$, an Ion-Acoustic wave can propagate with less Landau damping, and iii) $T_e/T_i > 3$, the Landau damping becomes even weaker because the phase velocity becomes much greater than the ion thermal speed. The Alfvén wave is a basic MHD-wave, which propagates along

the direction of the magnetic field and whose displacement is transverse to it. This wave is thought to be generated by the Kelvin-Helmholtz instability process, which results when magnetospheric plasma streams over another one. The combination of mechanical (pressure) and electromagnetic forces (charged particles) gives rise to different types of MHD waves, and the damping of these waves in the Ionosphere depends on the density of the neutral as well as the charged particles. MHD waves have lower frequency than the plasma frequency, and the latter is greater than the gyro (cyclotron) frequency, $f_{MHD} < \Omega < \nu_p$. If both the electric- and magnetic fields are neglected while the pressure dominates, we are talking about sound waves. If only the pressure is neglected while the electric and magnetic field dominates, we are talking about cold plasma waves, and finally, without neglecting any, we are talking about warm plasma waves. Waves in cold uniform magnetized plasma occur in the ion and electron cyclotron mode, leading to whistler waves. The electron cyclotron frequency is the characteristic wave frequency in magnetized plasma. At extremely low frequencies, both whistlers and ion-cyclotron waves become Alfvén waves.

4.8 Background of the Problem

The existence of plasma with two distinct types of hot & cold electrons has been reported earlier in the auroral Ionosphere. Waves in two-electron temperature plasma have been initiated by Jones et.al. [77]. A modified electron-acoustic mode exists in a plasma with two distinct hot and cold electron components [78]. Lichtenberg & Meuth [79] have observed hot electron instability in a mirror machine. Refractive ion-acoustic solitons in two-electron temperature plasma have been observed by Nishida

& Nagasawa [80]. The electron-acoustic and lower-hybrid waves of a multi-ion species plasma for the drift dissipative instabilities were investigated by M. Bose et.al. [81] , and found that the electron-acoustic drift dissipative instability appears at moderately high ion-viscosity and also found another electron-acoustic drift dissipative mode due to second ion species. The three-wave interaction process electron-acoustic wave (EAW), kinetic Alfvén wave and another electron acoustic waves are studied in the auroral region by using a multi-fluid approach [82]. In the linear limit, [83] sheared equilibrium flows can be the cause of instability of Alfvén-like electromagnetic waves and EAW in magnetospheric measurements. It is also shown that electromagnetic waves and sheared flows may cause the formation of a street vortex. Its size is sufficiently small than the scale lengths of the equilibrium density and velocity gradients. The linear mode structure of EAW have been studied for the modulational instability and rogue wave profiles also in four-component plasma system consisting of stationary ions, cold electron fluid, hot electrons and an electron beam. The dispersion relation obtained depends on various parameters such as beam density, beam velocity, beam temperature and non-extensivity q. Depending on the phase velocities, two electron-acoustic (EA) modes have been extracted, which are real. The nonlinearity and dispersion co-efficient affect the stability characteristics of EAW for both modes [84]. The lower hybrid instability is driven by cross-field currents in a density gradient in fairly narrow sheaths and is favoured by $T_i > T_e$ Both in the ionosphere and in fusion plasmas, the collisions and density inhomogeneity play an important role. Therefore, the drift-dissipative instabilities evolve in such plasmas. These instabilities have been studied in the frequency regime of $\omega < \omega_{ci}$

$k_z V_{\Theta i}$ and $V_{\Theta e}$ are ion-cyclotron frequency, ion & electron thermal velocities, respectively [85].

In this chapter, we have tried to investigate the effect of two different electron temperatures in an auroral Ionosphere where we have obtained a modified electron acoustic and a modified lower–hybrid drift dissipative mode under the same condition as Arefev (1970) [85] .

4.9 Dispersion Relations & Growth Rates calculation

In our calculations, we have considered the electrons as magnetized particles whereas the ions are un-magnetized. The magnetic field is considered to be along the z-direction. With the help of continuity equation, equation of motion and the Poisson's equation for each species, i.e. hot and cold electrons as well as ions, and following the steps mentioned in chapter 2 we obtained the expressions for the number densities for different types of particles as follows:

$$n_h = \frac{c}{\omega \beta_0}\left(\bar{k} \times \hat{z} \cdot \vec{\nabla} n_{0h}\right)\varphi + \frac{c}{\omega \beta_0} n_{0h} k_\perp \varphi - \frac{e n_{0h}}{m_e \omega^2} k^2 \varphi \qquad \textbf{(4.1)}$$

$$n_c = \frac{e n_{0c}}{m_e[\omega \omega_{ce} + k^2 V_{c\theta}]} k^2 \varphi \qquad \textbf{(4.2)}$$

$$n_i = \frac{e k^2 n_{0i}}{m_i \omega(\omega + i v_i)}\left[1 - \frac{kV}{\omega(\omega + i v_i)}\right]^{-1}\varphi \qquad \textbf{(4.3)}$$

where, the subscripts c, h, i, and θ represents the cold electrons, hot electrons, ions and thermal terms respectively. For the sake of simplification, we have neglected the viscosity terms. The collision frequency is neglected in comparison with the ion-cyclotron frequency.

The hot electrons satisfy the drift approximation to give

$$\frac{\partial^2 n_h}{\partial t^2} - \frac{c}{B_0} \frac{\partial}{\partial t} \left(\vec{\nabla}\varphi \times \vec{z} \right) \cdot \vec{\nabla} \cdot n_{0h} + \frac{c n_{0h}}{B_0 \omega_c} \frac{\partial^2}{\partial t^2} \nabla_\perp \varphi + \frac{e n_{0h}}{m_e} \frac{\partial^2 \varphi}{\partial t^2} = 0 \qquad \textbf{(4.4)}$$

Where, the electron temperature is neglected as the term containing temperature does not depend upon space.

Using equations (4.1), (4.2), (4.3), (4.4), along-with the Poisson's equation, we get,

$$\omega^2 k^2 \lambda_i^2 + \frac{n_{0h}}{n_{0i}} \left[\frac{\omega^2 k_\perp^2 T_i}{m_e \omega_{ce}^2} - \frac{T_i k_z^2}{m_e} - \omega \omega^* \right] + \frac{\omega^2 k^2 T_i}{m_e \left(\omega \omega_{ce} + k^2 V_{c\theta}^2 \right)} \frac{n_{0c}}{n_{0i}} -$$

$$\frac{\omega^2 k^2 T_i}{m_i \left(\omega \omega_{ci} - k^2 V_{i\theta}^2 \right)} = 0 \qquad \textbf{(4.5)}$$

here, $\omega^* = \frac{c(T_1 + T_2)}{e B_0} \frac{k_\perp}{L}$ is the ion drift velocity.

Considering the effect of cold electrons are very less as well as the system is dissipation-less and uniform, the dispersion relation equation (4.5) for single ion species reduces to

$$\omega^2 = \frac{C_s k_z^2}{b} \text{ and } \omega^2 = \frac{b}{a \omega_{pi}}$$

where, $a = k^2 \lambda_i^2 \alpha$, $c_s^2 = \frac{T_i}{m_e}$, $\alpha = 1 + \left(\frac{\omega_{pe}}{\omega_{ce}} \right)^2$, $b = \left(1 + \frac{m_i k_z^2}{m_e k_\perp^2} + a \right)$ at $T_i \gg$

T_e, & $\frac{m_i k_z^2}{m_e k_\perp^2} \ll 1$. We get the electron acoustic wave from the first root. Similarly, the lower hybrid wave can be obtained by considering $a \ll 1$ in the second root and the ion drift wave appears at $k_z \to 0$. Thus the dispersion relation given by equation (4.5) gives the electron acoustic, the lower-hybrid and the ion-drift wave.

Since we are interested in the dissipative and homogeneous density case, the dispersion relation for the modified electron acoustic wave is obtained as

$$\omega^2 = \frac{C_s{}^2 k_z^2 \left(\frac{n_{0h}}{n_{0i}}\right)}{1 + a + \frac{k_z^2 m_i n_{0h}}{k^2 m_e n_{0i}} + \frac{i v_i \omega^* n_{0h}}{k^2 V_{i\theta}{}^2 n_{0i}} + \frac{k^2 \lambda_i{}^2 \omega_{pc}^2}{\left(\omega_{ce}^2 - k^2 V_{c\theta}{}^2\right)}} \tag{4.6}$$

Here, the frequency of the excited wave is considered to be a complex quantity and can be expressed as, $\omega = \omega_r + i\gamma$ and the growth rate (γ) is obtained as

$$\gamma = \frac{|k_z| C_s \left(\frac{n_{0h}}{n_{0i}}\right)^{\frac{1}{2}} (S-1)^{\frac{1}{2}}}{\sqrt{2}\, S \left[1 + a + \frac{k_z^2 m_i n_{0h}}{k^2 m_e n_{0i}} + \frac{k^2 \lambda_i{}^2 \omega_{pc}^2}{\left(\omega_{ce}^2 - k^2 V_{c\theta}{}^2\right)}\right]^{1/2}} \tag{4.7}$$

where, $s = \left\{ 1 + \dfrac{v_i{}^2 (\omega^*)^2 \left(\frac{n_{0h}}{n_{0i}}\right)^2}{k^4 V_{\theta i}{}^4 \left[1 + a + \frac{k_z^2 m_i n_{0h}}{k^2 m_e n_{0i}} + \frac{k^2 \lambda_i{}^2 \omega_{pc}^2}{\left(\omega_{ce}^2 - k^2 V_{c\theta}{}^2\right)}\right]^2} \right\}^{\frac{1}{2}}$

In the absence of cold electron species, the relation for growth rate reduces to that given by Mohan & Yu [86], i.e.

$$\gamma = \frac{v_i |k_z| C_s \omega^*}{2\, k^2 V_{\theta i}{}^2 \left[1 + a + \frac{k_z^2 m_i}{k_\perp^2 m_e}\right]^{3/2}} \tag{4.9}$$

i.e. $\gamma = \dfrac{v_i |k_z| C_s \omega^*}{2\, k^2 V_{\theta i}{}^2 b^{3/2}}$

Now the dispersion relation for the lower hybrid drift dissipative instability, which is also modified due to the presence of the cold species of electrons, can be obtained from equation (5)

$$\omega^2 = \frac{k^2 V_{\theta i}{}^2 \left(1 + a + \frac{k^2 \lambda_i{}^2 \omega_{pe}^2}{\left(\omega_{ce}^2 - k^2 V_{c\theta}{}^2\right)}\right) + k_z^2 \lambda_i{}^2 \omega_{ph}^2 + i v_i \omega^* \left(\frac{n_{0h}}{n_{0i}}\right)}{\left[a + \frac{k^2 \lambda_i{}^2 \omega_{pc}^2}{\left(\omega_{ce}^2 - k^2 V_{c\theta}{}^2\right)}\right]} \tag{4.10}$$

And the growth rate is found to be

$$\gamma = \frac{kV_{\theta i}(S-1)^{\frac{1}{2}}\left[1+a+\frac{k_z^2 m_i n_{0h}}{k^2 m_e n_{0i}}+\frac{k^2 \lambda_i^2 \omega_{pe}^2}{\left(\omega_{ce}^2-k^2 V_{c\theta}^2\right)}\right]^{1/2}}{\sqrt{2}\, S\left(a+\frac{k^2 \lambda_i^2 \omega_{pe}^2}{\left(\omega_{ce}^2-k^2 V_{c\theta}^2\right)}\right)^{\frac{1}{2}}} \tag{4.11}$$

In absence of cold species of electrons with approximation equation (4.11) shows the expression for the lower hybrid wave.

$$\gamma = \frac{v_i \omega^*}{2b^{1/2}\alpha\omega_{pi}\,\lambda_i^2 k^2}$$

This expression for growth rate is also in agreement with one of the expression obtained by Mohan &Yu [86].

4.10 Discussion

Yu and Shukla [78] concluded, for unmagnetized plasma the evolved electron acoustic waves are strongly dependent to the number density of cold electrons. For drift dissipative case, the growth rate for electron acoustic wave equation (4.11) also depends on the number density of cold electrons, whereas this dependency is not that strong as shown by Yu and Shukla [78]. It was also shown that drift modes coupled with lower-hybrid and electron-acoustic waves become stable via ion collisional damping by the cold electrons but that unstable waves can exist when the electrons are warm [87]. Here, the calculation shows that the lower hybrid drift dissipative wave will not be affected much in the presence of cold electrons. In other words, the greater injection of high energetic particles in ionospheric plasma, generates the luminous glow of an electron acoustic drift dissipative wave, becomes unchanged. This

concludes that when the solar activity will be very high the aurora generates in ionosphere will affect more through the electron acoustic drift-dissipative wave.

4.11 Future plan

It is impossible to comprehend the entire dynamics while taking into account all impacts since different charge particles, dust, and neutral particles occur in the aurora at various temperatures. Different ionospheric models can be used to explore how auroral current systems affect the ionospheric plasma transport and plasma loss processes that are important to understand the auroral dynamics. It has already been done to formulate a mathematical model that uses a variation of the 5-moment approximation to describe the temporal evolution of density, drift, and temperature for five different ion species in two spatial dimensions [73]. Through a 2-D electrostatic treatment of the auroral currents, the fluid system is closed. To fully comprehend the interactions between ion heating, perpendicular transport, molecular ion production, this model can be expanded to include a few other particle types that can consider the natural uncontrolled situations.

Chapter 5

Effect of lower hybrid wave turbulence on the toroidal ITG mode in tokomak plasma

In fusion research the understanding of plasma confinement is one of the main task. Energy confinement must be strong enough to allow for a large number of reactions in order for this method to be economically viable. Reduced heat fluxes out of the plasma are required as a result of this process. The tokamak is the apparatus that has so far achieved the best achievements in terms of magnetic field-assisted plasma confinement. It is a torus-shaped vacuum chamber encircled by magnetic coils that produce a magnetic field that restricts the plasma.

Experimentally measured heat fluxes in tokamak plasmas are significantly higher than those that occur from collisions. The destabilization of low-frequency drift wave variations, which causes turbulence in the plasma on small scales relative to tokamak size, is largely responsible for this so-called anomalous transport.

Experimentally measured heat fluxes in tokamak plasmas are significantly higher than those that occur from collisions. The destabilization of low-frequency drift wave variations, which causes turbulence in the plasma on small scales relative to tokamak size, is largely responsible for this so-called anomalous transport.

The drift waves are collective modes of plasma oscillations that propagate through the plasma, arising as a result of the independent dynamics of ions and electrons in

the presence of temperature gradients of quantities describing the plasma in presence of the quasineutrality constraint. Ion Temperature Gradient (ITG) modes instabilities, i.e. electrostatic microinstabilities driven in the plasma by the presence of gradient in temperature of ions. This causes the transport of ion heat in suitable phase relation to yield an ion heat flux from center to edge. The main target of ion heat transport studies is to find ways to suppress or mitigate ITG modes, namely by increasing the threshold or reducing the stiffness level, in order to be able to achieve high core T_i values without having to rely on too high edge T_i values, which would raise plasma-wall interaction issues.

In this chapter we will study the effect of lower hybrid wave turbulence on the toroidal ion temperature gradient mode (ITG) i.e. $\eta_i = \frac{dln(T_i)}{dln(n)}$ in tokamak plasma. The energy source in ITG mode is the temperature gradient of the ions which coupled the drift like waves and ion acoustic waves aligned along the magnetic field. This mode plays a key role in the anomalous and thermal transport in tokamak [88]. ITG modes basically driven by negative compressibility $v_{T_i}^2(\frac{2}{3} - \eta_i)$ of ion motion. For the toroidal geometry this compressibility is affected by the compressible field ion motion whereas, in slab geometry the negative compressibility transform the ion acoustic oscillation into unstable compressional wave.

Theoreticians have focused a lot of attention from past few decades on the ion-temperature-gradient (ITG) driven turbulence, a subclass of gradient-driven turbulence [89] [90]. This is partially because, the primary thermal losses in big, neutral beam heated tokamaks occur on the ion channel. Ion losses in those systems

would therefore be adequately described by the analysis of different ITG turbulence model considering different perturbations. Also, drift modes driven by the ion temperature gradient mode have been subjects of wide theoretical research because of their relatively large growth rates. Before getting to the specific issue, several fundamental concepts are briefly covered to familiarize the reader with the subject. These concepts are covered in detail in any standard plasma physics textbook, therefore we won't get into those aspects here.

5.1 Magnetic confinement

The magnetic confinement theory makes use of the fact that the charged particles comprise the plasma are driven to follow paths along the magnetic field lines. Although the charged particles travel freely along the magnetic field, the Lorentz force causes them to gyrate in a path that is perpendicular to the field, known as the Larmor orbit. The characteristic scales of the gyromotion are the cyclotron frequency $\omega_{cj} = \frac{ZeB}{m_j}$ and the Larmor radius $\rho_j = \frac{\sqrt{T_j m_j}}{eBZ_j}$ where, j denoting the species of charges with the total charge Z_je, the mass, temperature and magnetic field are represented by m_j T_j and B, respectively.

5.2 Particle motions in a tokamak

The magnetic topology of a tokamak causes many drifts in charged particles. These drifts can be accurately computed in any textbook on plasma physics, thus we will briefly discuss them here. The particle dynamics is typically split into three parts: the

gyration motion, the fast parallel dynamics along the magnetic field lines and the slower drifts perpendicular to the field lines.

$$\vec{V} = \vec{V}_\perp + \vec{V}_\parallel + \vec{V}_{gyro}$$

The parallel velocity is of the order of the thermal velocity ($\vec{V}_\parallel = \sqrt{\frac{T_j}{m_j}}$), which is about 40 times larger for electrons than for protons. The perpendicular drift can be decomposed as the sum of the E $\times$B drift ($\vec{V}_{EXB}$), ∇B or magnetic drift ($\vec{V}_{\nabla B}$), curvature drift ($\vec{V}_R$) and the polarization drift ($\vec{V}_P$). The gyro velocity ($\vec{V}_{gyro}$) arises from time varying electric fields.

$$\vec{V}_\perp = \vec{V}_{EXB} + \vec{V}_{\nabla B} + \vec{V}_R + \vec{V}_P$$

The three first drifts can be expressed in the general form

$$\vec{V}_f = \frac{1}{q} \frac{\vec{F} \times \vec{B}}{B^2}$$

where, F is the force acting on the particle. Except the E $\times$ B drift, the rest of the drift velocities depend on the charge of the particle.

The particle drifts are indispensable components for understanding the plasma turbulence. The charge-dependent drifts induce a charge separation and therefore an electric field generates. Small perturbations may then be amplified due to E $\times$ B drift, resulting in instabilities and turbulent convection.

5.3 Neo-classical transport

The theory that describes the transport as driven purely by Coulomb collision but taking into account the toroidal effects is called neo-classical [91]. In a torus particles are subject to magnetic field inhomogeneity and curvature drifts that cause the particles with a low collision frequency to become trapped in the so-called "banana" orbits. Particles with a sufficiently large ratio between the velocities perpendicular and parallel to the magnetic field bounce between the points of high magnetic field. The plateau regime is characterized by a diffusion coefficient almost independent on the collisionality. In the Pfirsch-Schluter regime, that takes place for higher collision rates, the diffusion coefficient again increases with the collisionality. The transport increase can be explained using the random walk model. Because of the drifts due to the toroidal geometry, trapped particles drift off the flux surfaces with a radial excursion larger than the Larmor radius, increasing the collisional step size.
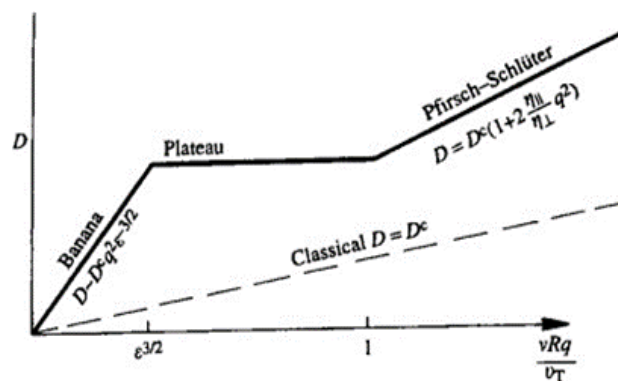

fig 5.1 Diffusion coefficient as a function of the normalized collision frequency [92]

5.4 Anomalous transport

Parallel transport is well described by the neo-classical theory: the experimental observations agree with the estimates for σ and B. However experiments don't confirm the estimates for cross-field diffusivities. In particular the ion heat diffusion coefficient exceeds neo-classical predictions up to one order of magnitude, and the electron diffusion coefficient by up to one or two orders of magnitude. Also the toroidal momentum diffusivity reaches values much larger than the neoclassical ones. Experiments give the most plausible explanation of the huge difference between the neo-classical estimates and the experimental results seems to be given by the collective nature of the plasma. The particles organize themselves as more or less coherent structures giving rise to collective modes, some of which may become unstable and lead to turbulent motions of the plasma. These turbulent processes influence significantly the mechanism of the transport. In many cases the turbulent contribution dominates the classical and neo-classical ones, and the transport is called anomalous. The collective modes can be divided in two classes: the magneto-hydrodynamics (MHD) modes, that are characterized by macroscopic dimensions, comparable to the plasma ones, and can be described by one fluid approach, and the drift waves, small scale phenomena in which electrons and ions must be described taking into account their disparate dynamics. MHD modes have to be maintained stable, because they cause macroscopic losses of plasma confinement. The plasma drift micro-instabilities don't lead to catastrophic events, as plasma disruptions, however they can give rise to enhanced particle and heat transport.

5.5 Magnetic Curvature-Drift Instability

In presence of either curvature or cross field transport, or also electron temperature gradient (ETG) a fluid instability occurs with growth rate $\gamma \sim \omega.^*$ The curvature drift frequency results from the temperature gradient-induced coupling of a tearing mode with $\omega \sim \omega^*$ and another mode with $\omega \sim \omega_c$ when driven by curvature. If the mode driven by cross field transport of particles or heat, the mode is basically a semi collisional tearing mode. We have completed a detailed analytic study of this instability using the linearized Braginskii fluid model [93] including diamagnetic effects, curvature drifts.

5.6 Trapped and passing particles

There are two types of charged particles in a tokamak: confined particles and passing particles. The charged particles in a tokamak experience a magnetic field that fluctuates between a maximum and a minimum value as they move parallel to the magnetic field lines. Thus, if certain particles have a velocity perpendicular to the magnetic field that is sufficiently greater than their parallel velocity, the magnetic field can function as a magnetic mirror, allowing some particles to reverse direction and be reflected back (or equivalently their energy sufficiently low). As a result, the particles are referred to as trapped whereas the particles which freely flow along the magnetic flied lines are named as passing. Different perpendicular diffusive transport is caused by trapped and passing particle movements. The condition for trapping can be expressed in terms of the particle energy

$$\varepsilon = \mu B \left(1 + \left(\frac{V_\parallel}{V_\perp} \right)^2 \right)$$

Here B and μ are the magnetic field and the magnetic momentum respectively.

5.7 Core plasma instabilities

The electrostatic ITG and the shorter wavelength electron-scale, ETG, respectively produced by ion or electron temperature gradients, those are the two primary core plasma instabilities in a tokamak that fall under the category of drift waves. The former takes into account both trapped and passing particles, whereas the latter solely takes into account the passing electrons. ITG and ETG instability have critical thresholds in temperature gradient and are also referred as, $\eta_{i,e}$, where, $\eta_{i,e} = \frac{L_n}{L_{T_{i,e}}}$ denotes the ratio of the density scale length to that of the ion and electron temperature. The ITG is generally the main instability responsible for ion heat transport in the plasma core. Correspondingly, ETG modes may produce large electron heat flux, on the electron scale. Trapped electrons can contribute to the drive of ITG modes, enhancing the ITG growth rate [94] [95], but they may also be the source of trapped electron modes (TEMs) [96]

5.8 RF ponderomotive force

Early days of fusion research considered the radiofrequency (RF) as tool for plasma confinement as because it can create the necessary plasma pressure, but these days RF is primarily utilised for heating and current drive. The effect of RF ponderomotive pressure has the stabilizing effect on the collisional, toroidal ITG mode by the local

radio frequency (RF) forces in the core region of the tokamak plasma flows. Furthermore, RF ponderomotive pressure on ITG mode in the collisional regime creates an inward particle flux.

The stability of low frequency modes in fusion machines is strongly influenced by radiofrequency (RF) waves as well. The RF fields may be used to control transport in many ways such as, by utilising the ponderomotive force of RF fields to stabilize the primary instabilities and to oppose the effects due to bad curvature of field lines [97], by introducing zonal flows with velocity shear with RF fields, [98] and by controlling test particle transport due to turbulence by Chaos control methods [99]

There are two effective components of local RF forces. The momentum absorption term and the parallel component of the resonant ponderomotive forces are the two functional elements of local RF forces, respectively [100]. The effects of the RF field can be entered only through the ponderomotive ion drift term to modify the growth rate expression through the continuity equation and ion energy equation.

5.9 Motivation of the work

For plasma confinement transport across the magnetic field is largely controlled by low frequency drift wave fluctuations [101]. In fusion plasmas the impurities decreases the quality of confinement by radiation energy loss and also contribute to the ITG driven instabilities which are considered to be one of the main cause for anomalous energy and particle transport. Therefore a significant theoretical and numerical investigations in plasma dynamics has been focused on the effects related with the development of the ion temperature gradient (ITG) mode instability in

connection with this confinement degradation [102]. Ion temperature gradient mode was first studied in slab geometry due to the pressure gradient term parallel to the ion motion in an inhomogeneous system [103] and gradually evolving to a mirror field in the Columbia Linear Machine (CLM). A new model of a hybrid ITG and trapped electron mode suggests that the magnetic curvature generates an extra drive for the mode and lowers its real frequency in the plasma frame [104]. The existence of a toroidal mode driven by solely ITG mode (η_i) effects was first pointed out by Horton et.al. [105]. Afterward it was investigated intensively [106]. Detailed study shows that toroidal effects give rise to higher η_i threshold compared to the slab case [88]F. Large amplitude lower hybrid waves in fusion devices is a central aspect of parametric instabilities. In the early years of fusion research, magnetic plasmas could be heated to thermonuclear temperatures using high power lower hybrid waves with frequencies between 500 MHz and 1 GHz. Recently, it was discovered that these waves were primarily active at higher frequencies (1–5 GHz) for driving non-inductive currents in tokamak plasmas. This opens the possibility of operating tokamak in steady state. Over the past three decades, there has been substantial study in the area of tokamak heating and current driving using radio frequency (RF) in the lower hybrid range of frequencies. In this frequency range, toroidal plasma current is sustained by refilling the collisional excitation of parametric instabilities [107]. The three wave parametric decay involve an ion cyclotron mode and a lower hybrid side band. Two stream instability oscillation is the most dominant process in the four wave coupling.

The analysis of a general ITG model can be found either from a low–frequency expansion of the general fluid equations [93] based on the drift velocity, or by using

the nonlinear gyrokinetic equation as a starting point [108]. For the improvement of the ITG instability, the ion temperature gradient is necessary to be combined with other effects such as the magnetic curvature, the parallel incompressibility or the presence of impurity species [109] etc.

In this chapter we try to observe the influence of radio frequency (RF) field in the ion energy transport using a two fluid model. The low frequency ITG mode (η_i) at ($\omega, \vec{k}$) with high frequency fast magnetosonic pump wave ($\omega_0, \vec{k}_0$) that generates side bands at ($\omega \pm \omega_0$, $k \pm k_0$). These side bands effect the primary RF wave and produce nonlinear density response that modifies the stability properties of ITG mode. Here the side bands are considered to be the electrostatic ion cyclotron waves. The effect of pondermotive force term is included in this calculation with the side band effect through the ion continuity equation and energy equation.

5.10 Formulation of Problem

We consider a nonlinear pump wave ($\omega_0, \vec{k}_0$) in the ion cyclotron frequency range to that propagates in the plasma with pressure gradient along x axis and an equilibrium magnetic field $\vec{B}$ along z direction. A local theory can be obtained that gives a detailed description since the fastest growing ITG mode (η_i) have the wavelengths that are much smaller than the background inhomogeneity scale lengths. The high amplitude electromagnetic RF pump waves produces an oscillatory drift velocity and density.

71

5.10.1 Equilibrium Condition

In equilibrium, at the presence of static magnetic field along z axis $B\hat{z}$, we consider LH waves($\Omega_i < \omega_0 < \Omega_e$, $\omega_0 > k_{0\perp}c_s$) spectrum of electrostatic potential of the form,

$$\varphi_0(\vec{r}, t) = \tilde{\phi}_0 \exp[-i(\omega_0 t - \vec{k}_0.\vec{r})]$$

where, $(\omega_0, \vec{k}_0)$ satisfies the dispersion relation

$$\omega^2 = \omega_{LH}^2 \left(1 + \frac{k_{0\parallel}^2}{k_{0\perp}^2} \frac{m_i}{m_e}\right)^{\frac{1}{2}}, \quad \omega_{LH}^2 = \frac{\omega_{pi}^2}{1 + \frac{\omega_{pe}^2}{\Omega_e^2}}$$

Here ω_{pe}, ω_{pi} are electron and ion plasma frequency and Ω_e is the electron cyclotron frequency.

In the presence of LH wave field, electrons and ions oscillating velocity

$$\vec{v}_{0e} = \left[i \frac{cT_e}{eB}\hat{z} \times \vec{k}_0 + \frac{cT_e}{eB}\frac{\omega_0}{\Omega_e}\vec{k}_{0\perp} - \frac{k_{0\parallel}c_e^2}{\omega_0}\hat{z}\right]\tilde{\phi}_0 \exp[-i(\omega_0 t - \vec{k}_0.\vec{r})] \qquad ;$$

where, $[\frac{cT_e}{eB} = \rho_e c_e = \rho_s c_s]$

$$= \left[i\rho_e c_e \hat{z} \times \vec{k}_0 + \omega_0 \rho_e^2 \vec{k}_{0\perp} - \frac{k_{0\parallel}c_e^2}{\omega_0}\hat{z}\right]\tilde{\phi}_0 \exp[-i(\omega_0 t - \vec{k}_0.\vec{r})]$$

$$v_{0\perp i} = \frac{k_{0\perp}c_s^2}{\omega_0}\tilde{\phi}_0 \exp[-i(\omega_0 t - \vec{k}_0.\vec{r})] \quad ; k_{0\perp} \gg k_{0\parallel}$$

The equilibrium electrons and ions density fluctuations, corresponding electrons and ions quiver velocities,

$$\tilde{n}_0 = \left[k_{0\perp}^2 \rho_e^2 - \frac{k_{0\parallel}^2 c_e^2}{\omega_0^2}\right]\tilde{\phi}_0 \exp[-i(\omega_0 t - \vec{k}_0.\vec{r})] \tag{5.1}$$

$$\tilde{n}_{0i} = \frac{k_{0\perp}^2 c_s^2}{\omega_0{}^2} \tilde{\phi}_0 \exp[-i(\omega_0 t - \vec{k}_0.\vec{r})] \tag{5.2}$$

Substituting equations (5.1) and (5.2) into Poisson's equation, we get

$$k_{0\perp}^2 \lambda_D^2 = \frac{k_{0\perp}^2 c_s^2}{\omega_0{}^2} - k_{0\perp}^2 \rho_e^2 + \frac{k_{0\parallel}{}^2 c_e^2}{\omega_0{}^2}$$

$$\omega_0^2 = \frac{c_s^2 \big/ \lambda_D^2}{\left(1 + \rho_e^2 \big/ \lambda_D^2\right)} \left(1 + \frac{k_{0\parallel}{}^2 m_i}{k_{0\perp}^2 m_e}\right) = \omega_{LH}^2 \left(1 + \frac{k_{0\parallel}{}^2 m_i}{k_{0\perp}^2 m_e}\right)^{\frac{1}{2}}$$

5.10.2 Driven mode the side bands LH wave dynamics

The low frequency mode ITG identified by the frequency ω_k and wave number $\vec{k}$. Interactions between ITG $(\omega_k, \vec{k})$ and LH waves pump $(\omega_0, \vec{k}_0)$ generate nonlinear ion density, velocity and potential fluctuations at the two side band wave scale $(\omega_1, \vec{k}_1)$ and $(\omega_2, \vec{k}_2)$.

where, $\omega_1 = \omega + \omega_0$; $\vec{k}_1 = \vec{k} + \vec{k}_0$; $\omega_2 = \omega - \omega_0$, $\vec{k}_2 = \vec{k} + \vec{k}_0$;

Ion dynamics of side band waves

In this section we present a brief description of ion dynamic in the lower-hybrid regime and calculate the perturbed number density of ions for the first and second ion side bands respectively.

First ion side band wave ($\omega_1, \vec{k}_1$)

$$\frac{\partial \vec{v}_{1\perp i}}{\partial t} = -c_s^2 \vec{\nabla}_\perp \phi_1 - \rho_e c_e [\hat{z} \times \vec{\nabla}\phi . \vec{\nabla} \vec{v}_{0\perp i} + \hat{z} \times \vec{\nabla}\phi_0 . \vec{\nabla} \vec{v}_{\perp i}] \tag{5.3}$$

$$\vec{v}_{1\perp i} = \frac{\vec{k}_{1\perp}c_s^2}{\omega_1}\,\phi_1 + i\,\frac{\rho_e c_e}{\omega_1}\left(\vec{k}\times\vec{k}_0\right).\hat{z}[\phi\vec{v}_{0\perp i} + \phi_0\vec{v}_{\perp i}] \tag{5.4}$$

Corresponding ion density perturbation

$$\frac{\partial n_{1i}}{\partial t} + \vec{\nabla}_\perp \vec{v}_{1\perp i} = -\rho_e c_e[\hat{z}\times\vec{\nabla}\phi.\vec{\nabla}\,n_{0i} + \hat{z}\times\vec{\nabla}\phi_0.\vec{\nabla}\,n_i] \tag{5.5}$$

$$n_{1i} - \frac{\vec{k}_{1\perp}\vec{v}_{1\perp i}}{\omega_1} = +i\,\frac{\rho_e c_e}{\omega_1}\left(\vec{k}\times\vec{k}_0\right).\hat{z}\,[\phi n_{0i} + \phi_0 n_i]$$

$$n_{1i} - \frac{k_{1\perp}^2 c_s^2}{\omega_1^2}\phi_1$$

$$= i\,\frac{\rho_e c_e}{\omega_1}\left(\vec{k}\times\vec{k}_0\right).\hat{z}\left[\phi\frac{\vec{k}_{1\perp}.\vec{v}_{0\perp i}}{\omega_1} - \phi_0\frac{\vec{k}_{1\perp}.\vec{v}_{\perp i}}{\omega_1}\right]$$

$$+ i\,\frac{\rho_e c_e}{\omega_1}\left(\vec{k}\times\vec{k}_0\right).\hat{z}\left[\frac{k_{0\perp}^2.c_s^2}{\omega_0^2} - 1\right]\phi_0\phi$$

for first ion side band wave $(\omega_1,\vec{k}_1)$ the ion perturbed density is

$$n_{1i} - \frac{k_{1\perp}^2 c_s^2}{\omega_1^2}\phi_1 = i\,\frac{\rho_e c_e}{\omega_1}\left(\vec{k}\times\vec{k}_0\right).\hat{z}\left[\frac{(\vec{k}_{1\perp}.\vec{k}_{0\perp})c_s^2}{\omega_1\omega_0} - i\rho_e c_e\frac{\vec{k}_{1\perp}.\left(\hat{z}\times\vec{k}\right)}{\omega_1}\right]\phi_0\phi$$

$$+ i\,\frac{\rho_e c_e}{\omega_1}\left(\vec{k}\times\vec{k}_0\right).\hat{z}\left[\frac{k_{0\perp}^2 c_s^2}{\omega_0^2} - 1\right]\phi_0\phi \tag{5.6}$$

here,

$$\vec{v}_{0\perp i} = \frac{\vec{k}_{0\perp}c_s^2}{\omega_0}\phi_0 \ , \ \ \vec{v}_{\perp i}\approx i\rho_e c_e\left(\hat{z}\times\vec{k}\right)\phi \ , \ \ n_{0i} = \frac{k_{0\perp}^2 c_s^2}{\omega_0^2}\,\phi_0 \ ,$$

$$n_i = n_e = \phi \ , \ k\ll k_0 \ , \ \omega\ll\omega_0$$

Second ion side band wave ($\omega_2,\ k_2$)

$$\frac{\partial \vec{v}_{2\perp i}}{\partial t} = -c_s^2 \vec{\nabla}_\perp \phi_2 - \rho_e c_e [\ \hat{z} \times \vec{\nabla}\phi.\vec{\nabla}\ \vec{v}^*_{0\perp i} + \hat{z} \times \vec{\nabla}\phi_0^{\ *}.\vec{\nabla}\ \vec{v}_{\perp i}]$$

$$\vec{v}_{2\perp i} = \frac{\vec{k}_{2\perp}c_s^2}{\omega_2}\ \phi_2 + i\ \frac{\rho_e c_e}{\omega_2}\ (\vec{k} \times \vec{k}_0).\hat{z}[\phi\vec{v}^*_{0\perp i} + \phi_0^{\ *}\vec{v}_{\perp i}]$$

Corresponding ion density perturbation

$$\frac{\partial n_{2i}}{\partial t} + \vec{\nabla}_\perp \vec{v}_{2\perp i} = -\rho_e c_e [\hat{z} \times \vec{\nabla}\phi.\vec{\nabla}\ n^*_{\ 0i} + \hat{z} \times \vec{\nabla}\phi_0^*.\vec{\nabla}\ n_i]$$

$$n_{2i} - \frac{\vec{k}_{2\perp}\vec{v}_{2\perp i}}{\omega_2} = -i\ \frac{\rho_e c_e}{\omega_1}\ (\vec{k} \times \vec{k}_0).\hat{z}\ [\phi n^*_{0i} + \phi_0^* n_i]$$

$$n_{2i} - \frac{k_{2\perp}^2 c_s^2}{\omega_2^2}\phi_2$$

$$= i\frac{\rho_e c_e}{\omega_2}\ (\vec{k} \times \vec{k}_0).\hat{z}\ \left[\phi \frac{\vec{k}_{2\perp}.\vec{v}^*_{0\perp i}}{\omega_2} - \phi_0^{\ *}\frac{\vec{k}_{2\perp}.\vec{v}_{\perp i}}{\omega_2}\right]$$

$$+ i\frac{\rho_e c_e}{\omega_2}\ (\vec{k} \times \vec{k}_0).\hat{z}\ \left[\frac{k_{0\perp}^{\ 2}.c_s^2}{\omega_0^2} - 1\right]\phi_0^*\phi$$

eplacing the values of $\vec{v}^*_{0\perp i}$ and $\vec{v}_{\perp i}$ in the second ion side band wave ($\omega_2, \vec{k}_2$) the ion

perturbed density becomes

$$n_{2i} - \frac{k_{2\perp}^2 c_s^2}{\omega_2^2}\phi_2$$

$$= -i\frac{\rho_e c_e}{\omega_2}\ (\vec{k} \times \vec{k}_0).\hat{z}\ \left[\frac{(\vec{k}_{2\perp}.\vec{k}_{0\perp})c_s^2}{\omega_2\omega_0} - i\rho_e c_e \frac{\vec{k}_{2\perp}.(\hat{z} \times \vec{k})}{\omega_2}\right]\phi_0^*\phi$$

$$+ i\frac{\rho_e c_e}{\omega_2}\ (\vec{k} \times \vec{k}_0).\hat{z}\ \left[\frac{k_{0\perp}^2 c_s^2}{\omega_0^2} - 1\right]\phi_0^*\phi$$

b. Electron dynamics of side band waves

First side band wave (ω_1, k_1):

Perpendicular electron drifts

The ExB drift, can be expressed as,

$$\vec{v}_{1E \times B} = \frac{c}{B} \, \hat{z} \times \vec{\nabla} \, \delta\phi_1 = \rho_e c_e \, \hat{z} \times \vec{\nabla}\phi_1$$

and, the Polarization drift can be expressed by,

$$\vec{v}_{1pol} = -\frac{c^2 m_e}{eB^2} \frac{d\delta\vec{E}_{1\perp}}{dt} = \rho_e^2 \frac{d\vec{\nabla}_\perp\phi_1}{dt} = \rho_e^2 \frac{\partial\vec{\nabla}_\perp\phi_1}{\partial t} + \rho_e^2 [\vec{v}_{E \times B}.\vec{\nabla}_\perp]\vec{\nabla}_\perp\phi$$

$$= \rho_e^2 \frac{\partial\vec{\nabla}_\perp\phi_1}{\partial t} + \rho_e^3 \, c_e [\hat{z} \times \vec{\nabla}\phi.\vec{\nabla}_\perp]\vec{\nabla}_\perp\phi \; -$$

$$= \rho_e^2 \frac{\partial\vec{\nabla}_\perp\phi_1}{\partial t} + \rho_e^3 \, c_e [(\hat{z} \times \vec{\nabla}\phi.\vec{\nabla}_\perp)\vec{\nabla}_\perp\phi_0 + (\hat{z} \times \vec{\nabla}\phi_0.\vec{\nabla}_\perp)\vec{\nabla}_\perp\phi \,]$$

$$\vec{\nabla}.\vec{v}_{1pol} = \rho_e^2 \frac{\partial\nabla_\perp^2\phi_1}{\partial t} + \rho_e^3 \, c_e [(\hat{z} \times \vec{\nabla}\phi.\vec{\nabla}_\perp)\nabla_\perp^2\phi_0 + (\hat{z} \times \vec{\nabla}\phi_0.\vec{\nabla}_\perp)\nabla_\perp^2\phi \,]$$

$$i\vec{k}_1.\vec{v}_{1pol} = i\omega_1\rho_e^2 k_{1\perp}^2\phi_1 + \rho_e^3 \, c_e (\vec{k} \times \vec{k}_0).\hat{z} \, (k_0^2 - k^2)\phi_0\phi$$

Parallel electron dynamics

$$\frac{\partial \vec{v}_{1\parallel e}}{\partial t} = c_e^2 \vec{\nabla}_\parallel \phi_1 - (\vec{v}_{E\times B}\vec{\nabla}.\vec{v}_{\parallel e}) = c_e^2 \vec{\nabla}_\parallel \phi_1 - \rho_e c_e [\,\hat{z}\times\vec{\nabla}\phi\vec{\nabla}.\vec{v}_{\parallel e}]$$

$$= c_e^2 \vec{\nabla}_\parallel \phi_1 - \rho_e c_e [\,\hat{z}\times\vec{\nabla}\phi.\vec{\nabla}v_{0\parallel e} + \hat{z}\times\vec{\nabla}\phi_0\vec{\nabla}.v_{\parallel e}]$$

$$\vec{v}_{1\parallel e} = -\frac{\vec{k}_{1\parallel}c_e^2}{\omega_1}\phi_1 + i\,\frac{\rho_e c_e}{\omega_1}\left(\vec{k}\times\vec{k}_0\right).\hat{z}[\phi\vec{v}_{0\parallel e} - \phi_0\vec{v}_{\parallel e}]$$

Corresponding electron density perturbation

$$\frac{\partial n_{1e}}{\partial t} + \vec{\nabla}_\perp.\vec{v}_{1\perp e} + \vec{\nabla}_\parallel.\vec{v}_{1\parallel e} = -\rho_e c_e[\hat{z}\times\vec{\nabla}\phi.\vec{\nabla}n_{0e} + \hat{z}\times\vec{\nabla}\phi_0.\vec{\nabla}n_e]$$

$$n_{1e} - \frac{\vec{k}_{1\perp}\vec{v}_{1\perp e}}{\omega_1} - \frac{\vec{k}_{1\parallel}\vec{v}_{1\parallel e}}{\omega_1} = i\,\frac{\rho_e c_e}{\omega_1}\left(\vec{k}\times\vec{k}_0\right).\hat{z}\,[\phi n_{0e} - \phi_0 n_e]$$

$$n_{1e} - \frac{\vec{k}_{1\perp}\vec{v}_{1\perp e}}{\omega_1} - \frac{\vec{k}_{1\parallel}\vec{v}_{1\parallel e}}{\omega_1} = i\,\frac{\rho_e c_e}{\omega_1}\left(\vec{k}\times\vec{k}_0\right).\hat{z}[\phi n_{0e} - \phi_0\phi]$$

here, we used the condition $n_e \sim n_i \sim \phi$

$$n_{1e} - k_{1\perp}^2\rho_e^2\phi_1 + i\,\frac{\rho_e^3\,c_e\left(\vec{k}\times\vec{k}_0\right).\hat{z}\,(k_0^2 - k^2)\phi_0\phi}{\omega_1} - \frac{k^2{}_{1\parallel}c_e^2}{\omega_1^2}\phi_1$$

$$- i\,\frac{\rho_e c_e\,\vec{k}_{1\parallel}}{\omega_1\,\omega_1}\left(\vec{k}\times\vec{k}_0\right).\hat{z}[\phi\vec{v}_{0\parallel e} + \phi_0\vec{v}_{\parallel e}]$$

$$= +i\,\frac{\rho_e c_e}{\omega_1}\left(\vec{k}\times\vec{k}_0\right).\hat{z}[\phi n_{0e} - \phi_0\phi]$$

for, ITG $\;{}^{\omega}\!/_{k_\parallel c_e} \ll 1$, $\lambda_f \gg qR\;$ this yields $n_e \sim n_i \sim \phi\;$ and $\;v_{\parallel e}\approx 0$ and

$$\vec{v}_{0\parallel e} = -\frac{\vec{k}_{0\parallel}c_e^2}{\omega_0}\hat{z}\,\tilde{\phi}_0\;,\; n_{0e} = [k_{0\perp}^2\rho_e^2 - \frac{k_{0\parallel}{}^2 c_e^2}{\omega_0^2}]\tilde{\phi}_0$$

$$n_{1e} - k_{1\perp}^2 \rho_e^2 \phi_1 + i \frac{\rho_e^3 \, c_e (\vec{k} \times \vec{k}_0).\hat{z}\,(k_0^2 - k^2)\phi_0\phi}{\omega_1} - \frac{k^2{}_{1\parallel} c_e^2}{\omega_1{}^2} \phi_1$$

$$- i \, \frac{\rho_e c_e}{\omega_1} \frac{\vec{k}_{1\parallel}.\vec{k}_{0\parallel} c_e^2}{\omega_0 \omega_1} (\vec{k} \times \vec{k}_0).\hat{z}[\phi\phi_0]$$

$$= +i \, \frac{\rho_e c_e}{\omega_1} (\vec{k} \times \vec{k}_0).\hat{z}[k_{0\perp}^2 \rho_e^2 - \frac{k_{0\parallel}{}^2 c_e^2}{\omega_0{}^2} - 1]\phi_0\phi$$

$$(5.8)$$

Second side band wave (ω_2, k_2)

Perpendicular electron drifts or, E x B drift

$$\vec{v}_{2E\times B} = \frac{c}{B} \, \hat{z} \times \vec{\nabla} \, \delta\phi_2 = \rho_e c_e \, \hat{z} \times \vec{\nabla} \phi_2$$

The polarization drift

$$\vec{v}_{2pol} = -\frac{c^2 m_e}{eB^2} \frac{d\delta\vec{E}_{2\perp}}{dt} = \rho_e^2 \frac{d\vec{\nabla}_\perp \phi_2}{dt} = \rho_e^2 \frac{\partial\vec{\nabla}_\perp \phi_2}{\partial t} + \rho_e^2 [\vec{v}_{E\times B}.\vec{\nabla}_\perp]\vec{\nabla}_\perp \phi$$

$$= \rho_e^2 \frac{\partial\vec{\nabla}_\perp \phi_2}{\partial t} + \rho_e^3 \, c_e [\hat{z} \times \vec{\nabla}\phi.\vec{\nabla}_\perp]\vec{\nabla}_\perp \phi$$

$$= \rho_e^2 \frac{\partial\vec{\nabla}_\perp \phi_2}{\partial t} + \rho_e^3 \, c_e [(\hat{z} \times \vec{\nabla}\phi.\vec{\nabla}_\perp)\vec{\nabla}_\perp \phi_0^* + (\hat{z} \times \vec{\nabla}\phi_0^*.\vec{\nabla}_\perp)\vec{\nabla}_\perp \phi]$$

$$\vec{\nabla}.\vec{v}_{2pol} = \rho_e^2 \frac{\partial\nabla_\perp^2 \phi_2}{\partial t} + \rho_e^3 \, c_e [(\hat{z} \times \vec{\nabla}\phi.\vec{\nabla}_\perp)\nabla_\perp^2 \phi_0^* + (\hat{z} \times \vec{\nabla}\phi_0^*.\vec{\nabla}_\perp)\nabla_\perp^2 \phi]$$

$$i\vec{k}_2.\vec{v}_{2pol} = i\omega_2 \rho_e^2 k_{2\perp}^2 \phi_2 - \rho_e^3 \, c_e (\vec{k} \times \vec{k}_0).\hat{z}\,(k_0^2 - k^2)\phi_0^*\phi$$

Parallel electron dynamics

$$\frac{\partial\vec{v}_{2\parallel e}}{\partial t} = c_e^2 \vec{\nabla}_\parallel \phi_2 - (\vec{v}_{E\times B}\vec{\nabla}.\vec{v}_{\parallel e}) = c_e^2 \vec{\nabla}_\parallel \phi_2 - \rho_e c_e [\hat{z} \times \vec{\nabla}\phi.\vec{\nabla} v_{\parallel e}]$$

$$= c_e^2 \vec{\nabla}_\parallel \phi_2 - \rho_e c_e [\, \hat{z} \times \vec{\nabla}\phi . \vec{\nabla}\vec{v}^*_{0\parallel e} + \hat{z} \times \vec{\nabla}\phi_0^* . \vec{\nabla}v_{\parallel e}]$$

$$\vec{v}_{2\parallel e} = -\frac{\vec{k}_{2\parallel} c_e^2}{\omega_2}\, \phi_2 - i\, \frac{\rho_e c_e}{\omega_2}\, (\vec{k} \times \vec{k}_0).\hat{z}[\phi \vec{v}^*_{0\parallel e} - \phi_0^* \vec{v}_{\parallel e}]$$

Corresponding electron density perturbation

$$\frac{\partial n_{2e}}{\partial t} + \vec{\nabla}_\perp . \vec{v}_{2\perp e} + \vec{\nabla}_\parallel . \vec{v}_{2\parallel e} = -\rho_e c_e [\hat{z} \times \vec{\nabla}\phi . \vec{\nabla} n_{0e}^* + \hat{z} \times \vec{\nabla}\phi_0^* . \vec{\nabla} n_e]$$

$$n_{2e} - \frac{\vec{k}_{2\perp} \vec{v}_{2\perp e}}{\omega_2} - \frac{\vec{k}_{2\parallel} \vec{v}_{2\parallel e}}{\omega_2} = -i\, \frac{\rho_e c_e}{\omega_2}\, (\vec{k} \times \vec{k}_0).\hat{z}\, [\phi n_{0e}^* - \phi_0^* n_e]$$

$$n_{2e} - \frac{\vec{k}_{2\perp} \vec{v}_{2\perp e}}{\omega_2} - \frac{\vec{k}_{2\parallel} \vec{v}_{2\parallel e}}{\omega_2} = -i\, \frac{\rho_e c_e}{\omega_2}\, (\vec{k} \times \vec{k}_0).\hat{z}\, [\phi n_{0e}^* - \phi_0^* \phi]$$

here we used the condition $n_e \sim n_i \sim \phi$

$$n_{2e} - k_{2\perp}^2 \rho_e^2 \phi_2 - i\, \frac{\rho_e^3\, c_e (\vec{k} \times \vec{k}_0).\hat{z}\, (k_0^2 - k^2)\phi_0^* \phi}{\omega_2} - \frac{k^2{}_{2\parallel} c_e^2}{\omega_2^2}\, \phi_2$$

$$+ i\, \frac{\rho_e c_e}{\omega_2} \frac{\vec{k}_{2\parallel}}{\omega_2}\, (\vec{k} \times \vec{k}_0).\hat{z}\, [\phi v^*_{0\parallel e} - \phi_0^* \vec{v}_{\parallel e}]$$

$$= -i\, \frac{\rho_e c_e}{\omega_2}\, (\vec{k} \times \vec{k}_0).\hat{z}[\phi n_{0e}^* - \phi_0^* \phi]$$

for, ITG $\quad {}^{\omega}\!/_{k_\parallel c_e} \ll 1$, $\lambda_f \gg qR$ this yields $n_e \sim n_i \sim \phi$ and

$v_{\parallel e} \approx 0$ and

$$\vec{v}_{0\parallel e} = -\frac{\vec{k}_{0\parallel} c_e^2}{\omega_0} \hat{z}\, \tilde{\phi}_0 , \quad n_{0e} = [k_{0\perp}^2 \rho_e^2 - \frac{k_{0\parallel}{}^2 c_e^2}{\omega_0^2}]\tilde{\phi}_0$$

$$n_{2e} - k_{2\perp}^2 \rho_e^2 \phi_2 - i \frac{\rho_e^3 \, c_e (\vec{k} \times \vec{k}_0).\hat{z} \, (k_0^2 - k^2) \phi_0^* \phi}{\omega_2} - \frac{k^2_{2\parallel} c_e^2}{\omega_2^2} \phi_2$$

$$- i \frac{\rho_e c_e}{\omega_2} \frac{\vec{k}_{2\parallel}}{\omega_2} \frac{\vec{k}_{0\parallel} c_e^2}{\omega_0} (\vec{k} \times \vec{k}_0).\hat{z} \, [\phi \phi_0^*]$$

$$= -i \frac{\rho_e c_e}{\omega_2} (\vec{k} \times \vec{k}_0).\hat{z} [k_{0\perp}^2 \rho_e^2 - \frac{k_{0\parallel}^2 c_e^2}{\omega_0^2} - 1] \phi_0^* \phi$$

(5.9)

To find the side band potentials we apply the Poisson's equation

$$-\lambda_D^2 k_{1\perp}^2 \phi_1 = n_{1i} - n_{1e}$$

$$-\lambda_D^2 k_{2\perp}^2 \phi_2 = n_{2i} - n_{2e}$$

Substituting the values of (5.6), (5.8), (5.7) and (5.9) in the above equations we get the side potentials of the following form.

$$\phi_{1,2} = F(\phi_{ITG}) \begin{pmatrix} \dfrac{\phi_0}{\varepsilon_1} \\ \dfrac{\phi_0^*}{\varepsilon_2} \end{pmatrix}$$

$$n_{1i} = \frac{k_{1\perp}^2 c_s^2}{\omega_1^2} \phi_1 + i \frac{\rho_e c_e}{\omega_1} (\vec{k} \times \vec{k}_0).\hat{z} \left[\frac{(\vec{k}_{1\perp}.\vec{k}_{0\perp}) c_s^2}{\omega_1 \omega_0} - i\rho_e c_e \frac{\vec{k}_{1\perp}.(\hat{z} \times \vec{k})}{\omega_1} \right] \phi_0 \phi$$

$$+ i \frac{\rho_e c_e}{\omega_1} (\vec{k} \times \vec{k}_0).\hat{z} \left[\frac{k_{0\perp}^2 c_s^2}{\omega_0^2} - 1 \right] \phi_0 \phi$$

$$-n_{1e} = -k_{1\perp}^2 \rho_e^2 \phi_1 + i\frac{\rho_e^3 c_e (\vec{k} \times \vec{k}_0).\hat{z} \,(k_0^2 - k^2)\phi_0 \phi}{\omega_1} - \frac{k^2{}_{1\parallel} c_e^2}{\omega_1{}^2}\,\phi_1$$

$$- i\frac{\rho_e c_e}{\omega_1}\frac{\vec{k}_{1\parallel}.\vec{k}_{0\parallel} c_e^2}{\omega_0 \omega_1}\,(\vec{k} \times \vec{k}_0).\hat{z}[\phi \phi_0] - i\frac{\rho_e c_e}{\omega_1}(\vec{k} \times \vec{k}_0).\hat{z}[k_{0\perp}^2 \rho_e^2$$

$$- \frac{k_{0\parallel}{}^2 c_e^2}{\omega_0{}^2} - 1]\phi_0 \phi$$

now,

$$-\lambda_D^2 k_{1\perp}^2 \phi_1 = n_{1i} - n_{1e}$$

$$-\lambda_D^2 k_{1\perp}^2 \phi_1 = \left(\frac{k_{1\perp}^2 c_s^2}{\omega_1^2} - k_{1\perp}^2 \rho_e^2 - \frac{k^2{}_{1\parallel} c_e^2}{\omega_1{}^2}\right)\phi_1 + i\frac{\rho_e c_e}{\omega_1}(\vec{k} \times \vec{k}_0).\hat{z}\,[\frac{(\vec{k}_{1\perp}.\vec{k}_{0\perp})c_s^2}{\omega_1 \omega_0}$$

$$- i\rho_e c_e \frac{\vec{k}_{1\perp}.(\hat{z} \times \vec{k})}{\omega_1} + \left(\frac{k_{0\perp}^2 c_s^2}{\omega_0^2} - 1\right) + \rho_e^2\,(k_0^2 - k^2) - \frac{\vec{k}_{1\parallel}.\vec{k}_{0\parallel} c_e^2}{\omega_0 \omega_1}$$

$$- (k_{0\perp}^2 \rho_e^2 - \frac{k_{0\parallel}{}^2 c_e^2}{\omega_0{}^2} - 1)]\phi_0 \phi$$

$$[-\lambda_D^2 k_{1\perp}^2 - \frac{k_{1\perp}^2 c_s^2}{\omega_1^2} + k_{1\perp}^2 \rho_e^2 + \frac{k^2{}_{1\parallel} c_e^2}{\omega_1{}^2}]\phi_1$$

$$= i\frac{\rho_e c_e}{\omega_1}(\vec{k} \times \vec{k}_0).\hat{z}\,[\frac{(\vec{k}_{1\perp}.\vec{k}_{0\perp})c_s^2}{\omega_1 \omega_0} - i\rho_e c_e \frac{\vec{k}_{1\perp}.(\hat{z} \times \vec{k})}{\omega_1}$$

$$+ \left(\frac{k_{0\perp}^2 c_s^2}{\omega_0^2} - 1\right) + \rho_e^2\,(k_0^2 - k^2) - \frac{\vec{k}_{1\parallel}.\vec{k}_{0\parallel} c_e^2}{\omega_0 \omega_1} - (k_{0\perp}^2 \rho_e^2 - \frac{k_{0\parallel}{}^2 c_e^2}{\omega_0{}^2}$$

$$- 1)]\phi_0 \phi$$

$$\phi_1 = \frac{i\frac{\rho_e c_e}{\omega_1}\left(\vec{k}\times\vec{k}_0\right).\hat{z}\left[\frac{(\vec{k}_{1\perp}.\vec{k}_{0\perp})c_s^2}{\omega_1\omega_0} - i\rho_e c_e\frac{\vec{k}_{1\perp}.\left(\hat{z}\times\vec{k}\right)}{\omega_1} + \left(\frac{k_{0\perp}^2 c_s^2}{\omega_0^2} - 1\right) + \rho_e^2\,(k_0^2 - k^2) - \frac{\vec{k}_{1\parallel}.\vec{k}_{0\parallel}c_e^2}{\omega_0\omega_1} - (k_{0\perp}^2\rho_e^2 - \frac{k_{0\parallel}^2 c_e^2}{\omega_0^2} - 1)\right]}{-\lambda_D^2 k_{1\perp}^2 - \frac{k_{1\perp}^2 c_s^2}{\omega_1^2} + k_{1\perp}^2\rho_e^2 + \frac{k_{1\parallel}^2 c_e^2}{\omega_1^2}}\,\phi_0\phi$$

$$\phi_1 = \phi_{ITG}\left(\frac{\phi_0}{\epsilon}\right)$$

again

$$n_{2i} = \frac{k_{2\perp}^2 c_s^2}{\omega_2^2}\phi_2 - i\frac{\rho_e c_e}{\omega_2}\left(\vec{k}\times\vec{k}_0\right).\hat{z}\left[\frac{(\vec{k}_{2\perp}.\vec{k}_{0\perp})c_s^2}{\omega_2\omega_0} - i\rho_e c_e\frac{\vec{k}_{2\perp}.\left(\hat{z}\times\vec{k}\right)}{\omega_2}\right]\phi_0^*\phi$$

$$+ i\frac{\rho_e c_e}{\omega_2}\left(\vec{k}\times\vec{k}_0\right).\hat{z}\left[\frac{k_{0\perp}^2 c_s^2}{\omega_0^2} - 1\right]\phi_0^*\phi$$

$$n_{2e} = +k_{2\perp}^2\rho_e^2\phi_2 + i\frac{\rho_e^3 c_e\left(\vec{k}\times\vec{k}_0\right).\hat{z}\,(k_0^2 - k^2)\phi_0^*\phi}{\omega_2} + \frac{k_{2\parallel}^2 c_e^2}{\omega_2^2}\,\phi_2$$

$$+ i\,\frac{\rho_e c_e}{\omega_2}\frac{\vec{k}_{2\parallel}}{\omega_2}\frac{\vec{k}_{0\parallel}c_e^2}{\omega_0}\left(\vec{k}\times\vec{k}_0\right).\hat{z}\,[\phi\phi_0^*] - i\,\frac{\rho_e c_e}{\omega_2}\left(\vec{k}\times\vec{k}_0\right).\hat{z}[k_{0\perp}^2\rho_e^2$$

$$- \frac{k_{0\parallel}^2 c_e^2}{\omega_0^2} - 1]\phi_0^*\phi$$

$$-\lambda_D^2 k_{2\perp}^2\boldsymbol{\phi_2} = \boldsymbol{n_{2i}} - \boldsymbol{n_{2e}}$$

$$\left(-\lambda_D^2 k_{2\perp}^2 - \frac{k_{2\perp}^2 c_s^2}{\omega_2^2} + k_{2\perp}^2 \rho_e^2 + \frac{k^2_{2\parallel} c_e^2}{\omega_2^2}\right)\phi_2$$

$$= -i\frac{\rho_e c_e}{\omega_2}\left(\vec{k}\times\vec{k}_0\right).\hat{z}\left[\frac{(\vec{k}_{2\perp}.\vec{k}_{0\perp})c_s^2}{\omega_2\omega_0} - i\rho_e c_e\frac{\vec{k}_{2\perp}.\left(\hat{z}\times\vec{k}\right)}{\omega_2}\right.$$

$$+\left(\frac{k_{0\perp}^2 c_s^2}{\omega_0^2} - 1\right) + \rho_e^2\left(k_0^2 - k^2\right) - \frac{\vec{k}_{2\parallel}\vec{k}_{0\parallel}c_e^2}{\omega_2\,\omega_0}$$

$$\left.-\left(k_{0\perp}^2\rho_e^2 - \frac{k_{0\parallel}^2 c_e^2}{\omega_0^2} - 1\right)\right]\phi_0^*\phi$$

$\phi_2 =$

$$\frac{\begin{aligned}&i\frac{\rho_e c_e}{\omega_2}\left(\vec{k}\times\vec{k}_0\right).\hat{z}\,[\frac{(\vec{k}_{2\perp}.\vec{k}_{0\perp})c_s^2}{\omega_2\omega_0} - i\rho_e c_e\frac{\vec{k}_{2\perp}.\left(\hat{z}\times\vec{k}\right)}{\omega_2} + \left(\frac{k_{0\perp}^2 c_s^2}{\omega_0^2} - 1\right)\\&+\rho_e^2\left(k_0^2 - k^2\right) - \frac{\vec{k}_{2\parallel}\vec{k}_{0\parallel}c_e^2}{\omega_2\,\omega_0} - \left(k_{0\perp}^2\rho_e^2 - \frac{k_{0\parallel}^2 c_e^2}{\omega_0^2} - 1\right)]\end{aligned}}{\left(-\lambda_D^2 k_{2\perp}^2 - \frac{k_{2\perp}^2 c_s^2}{\omega_2^2} + k_{2\perp}^2 \rho_e^2 + \frac{k^2_{2\parallel} c_e^2}{\omega_2^2}\right)}\phi_0^*\phi$$

$$\phi_2 = \phi_{ITG}\left(\frac{\phi_0^*}{\epsilon}\right)$$

5.11 Toroidal ITG and trapped electron mode

To obtain linear dispersion relation, we shall drop all nonlinear terms and assume that

the all the perturbed quantities n, T, v_s and φ proportional to

$$\varphi(\vec{r}, t) = \exp[-i\left(\omega t - \vec{k}.\vec{r}\right)]$$

A set of fluid equations is used to describe a collisionless toroidal ITG turbulence

Applying the continuity equation,

$$\frac{\partial n_{ik}}{\partial t} + \vec{\nabla}. \left[n_{ik} \left(\vec{v}_{Ek} + \vec{v}_{*pk} + \vec{v}_{pk} \right) \right]$$

$$= -\vec{\nabla}. \left[n_{1i} \vec{v}_{0i}^* + n_{0i}^* \vec{v}_{1i} \right] + \vec{\nabla}. \left[n_{2i} \vec{v}_{0i}^* + n_{0i}^* \vec{v}_{2i} \right] - \vec{\nabla}. v^{nl}$$

(5.10)

These drift velocities at ITG scale (ω, k) are due to $\vec{E} \times \vec{B}$ drift $(\vec{v}_E)$, ion diamagnetic drift $(\vec{v}_{*p})$, and ion polarization drift $(\vec{v}_p)$ respectively.

$$\vec{v}_{Ek} = \frac{c}{B^2} \left(\vec{B} \times \vec{\nabla}. \delta \varphi_k \right),$$

$$\vec{v}_{*pik} = \frac{c}{en_i B^2} \left(\vec{B} \times \vec{\nabla}. \delta p_{ik} \right),$$

$$\vec{v}_{pik} = \frac{\vec{c}}{B\Omega_i} \left[\partial_t + \left(\vec{v}_{Ek} + \vec{v}_{*pik} \right) \nabla_\perp \varphi_k, \right.$$

here the ion polarization term gives the first order FLR terms.in the equation (5.10) the last two terms represent the side band coupling due to the influence of pondermotive force. In the limit $k^2 \rho^2 > 0.1$ the parallel ion motion is neglected for toroidal η_i mode which corresponds to the fastest growing modes.

The continuity equation (5.10) can further be simplified to,

$$\partial \tilde{n}_{ik} - \rho_s^2 \left(\partial_t + \alpha_i v_* \nabla_y \right) \nabla_\perp^2 \tilde{\varphi}_k - \varepsilon_n v_* \nabla_y \left(\tilde{\varphi}_k + \tau \tilde{n}_k + \tau \tilde{T}_{ik} + s_1 + s_2 = 0 \quad \textbf{(5.11)}$$

$$s_1 = \vec{\nabla}. \left[n_{1i} \vec{v}_{0i}^* + n_{0i}^* \vec{v}_{1i} \right] + \vec{\nabla}. \left[n_{2i} \vec{v}_{0i}^* + n_{0i}^* \vec{v}_{2i} \right]$$

$$s_2 = \vec{\nabla}. v^{nl}$$

$$v_{i\perp} = \frac{k_{1\perp} c_s^2}{\omega_1} \phi_1 + i \frac{\rho_e c_e}{\omega_1} \left(\vec{k} \times \overrightarrow{k_0} \right). \hat{z} \left[\phi \vec{v}_{0\perp i} - \phi_0 \vec{v}_{\perp i} \right]$$

$$\alpha_i = 1 + \eta_i \,,$$

$\tau = \frac{T_i}{T_e}$, τ denotes the ratio of ion to electron temperature,

$c_s^2 = \frac{T_e}{m_i}$, c_s is the ion sound velocity

The coupling to the energy equation is given by,

$$\vec{\nabla}.(n_i \vec{v}_{*i}) = \vec{v}_{Di}.\vec{\nabla}.\delta p_i$$

where, $\vec{v}_{Di}$ is the sum of the curvature drift and magnetic drift ($\vec{\nabla}B$)

The lowest order finite Larmor effect (FLR) can be obtained by substituting the perturbed part of $\vec{v}_{*pi}$ in $\frac{\partial v}{\partial t}$ in $\vec{v}_{pi}$ and the energy equation considering all curvature effect can be expressed as,

$$\frac{3}{2}\, n_i \left(\frac{\partial}{\partial t} + \vec{v}_i.\vec{\nabla}\right) T_i + p_i.\vec{\nabla}\vec{v}_i = -\vec{\nabla}\vec{q}_{*i} \qquad (5.12)$$

where, n and v is obtained from the continuity equation , $\vec{q}_{*i}$ is the diamagnetic heat flux.

$$\vec{\nabla}\vec{q}_{*i} = -\frac{5}{2}n_i\vec{v}_{*i}.\vec{\nabla}T_i + \frac{5}{2}n_i\vec{v}_{Di}.\vec{\nabla}T_i$$

Ion energy equation:

$$\frac{d\tilde{T}_i}{dt} - \frac{5\tau_i}{3}\varepsilon_n v_{*e}\nabla_y\tilde{T}_i + \left(\eta_i - \frac{2}{3}\right)v_{*e}\nabla_y\tilde{\varphi} - \frac{2}{3}\frac{d\tilde{n}}{dt} = 0 \qquad (5.13)$$

5.12 Linear and nonlinear Dispersion Relation.

The dispersion relation for the toroidal ITG instability can be determined by the linearizing the equations (5.11) to (5.13) and by applying the Fourier expansion to the perturbed quantities we get the linear density response [110].

$$\frac{\delta n_i}{n} = \frac{\omega_{*e} + \tau\omega_{Di} + \tau\left(\frac{2}{3} - \eta_i\right)\omega_{*i}\delta - k^2\rho_s{}^2[\omega - \omega_{*i}\delta(1 + \eta_i)]}{\omega - \frac{5}{3}\omega_{Di}\left(1 + \frac{2}{3}\eta_i\right)}$$

here, $\delta = \frac{\omega_{Di}}{\omega - \frac{5}{3}\omega_{Di}}$ arises due to the diamagnetic heat flow, ω_{*e} is the electron diamagnetic drift frequency, and ω_{Di} is the magnetic drift frequency.

The nonlinear density response considering the contribution of all the term from the equations (5.11) to (5.13) gives the following expression

$$\left(\frac{\delta n_i}{n_0}\right)_{nonlinear} = \left(\frac{e\phi}{T_e}\right)\frac{[\omega_{Di}\frac{\delta T_i}{T_{i0}} + \vec{k}.\vec{v}^{nl} + 0.51\frac{\vec{k}}{n_0}.[n_{1i}\vec{v}^*_{0i} + n^*_{0i}\vec{v}_{1i} + n_{2i}\vec{v}^*_{0i} + n^*_{0i}\vec{v}_{2i}]}{\omega - \frac{5}{3}\omega_{Di}\left(1 + \frac{2}{3}\eta_i\right)}$$

The initial phase of the ITG instability is characterized by the growth rate of the linearly unstable modes, which is confirmed by the linear excitation of the ITG modes. This shows the development of radial patterns of the fluctuating potential and temperature that propagate along the poloidal direction with their characteristic group velocity [111]. From the nonlinear density relation the stabilizing effect on the η_i mode corresponding to mode propagation in the ion diamagnetic direction need to be calculated and also the variation of growth rate and susceptibility (χ_i) with permeability ε_n under certain parameters are yet to be studied graphically.

5.12 Discussion and Future Plan

Improving the characterization and comprehension of momentum transport and plasma rotation is a key objective in tokamak fusion research. Finding how impurities affect tokamak performance by contributing to radiation losses in reduced fusion power is an important additional study. By taking into account the trapped electrons, we are attempting to examine the impact of impurity ions on the ITG driven modes in toroidal plasma in this problem. Here, we have calculated the electron and ion perturbed side band potential and number densities. Next, we have calculated the linear density response, which provides the linear dispersion relation. The dispersion relation in the presence of radio frequency fields in the lower hybrid range of frequencies gives the nonlinear density response. The drift wave's eigenfrequency is thought to be modified by the parametric coupling between the pump wave and ITG, which results in sideband waves in the lower hybrid range of frequencies that impose a ponderomotive force on electrons and affect the growth rate.

Chapter-6

Conclusion

In this thesis, my investigations are concerned with the observation of drift waves in the low-frequency domain. Here, three distinct cases of drift instabilities are concerned. For solving these problems we consider different assumptions. In the third chapter I try to study the effect of sheared magnetic field on ions in a collisional plasma with density gradient also the stabilization of the mode using fluid model. The analysis is done in a sheared slab geometry. In the fifth chapter I try to extend this work, by taking a plasma system where the ion temperature gradient is present and solve it in toroidal geometry along with this the effect RF pump is also considered which generates two side bands due to pondermotive force, but to avoid the complexity the plasma is considered collisionless in this case. In chapter four, I try to study the coupling effect of lower hybrid drift wave and the ion acoustic wave for multi species, i.e. cold electrons, hot electrons and ions present in auroral plasma. Though here we consider the collisions between the species but consider a simple constant magnetic field along z axis. All the derivations are done using fluid model.

 As plasma is a complex system with different nonlinear effects, it is impossible to give an exact model considering all effects. Here, we try to do all the derivations using a fluid model focusing on few effects in different problems. This work can be extended by allowing other effects.

Bibliography

[1] A. Piel, Plasma physics: an introduction to laboratory, space, and fusion plasmas, New York: Springer, 2017.

[2] T. H. Stix, Waves in plasmas, New York: Springer Science & Business Media, 1992.

[3] D. Swanson, Plasma waves, CRC Press, 2003.

[4] T. H. Stix and R. W. Palladino, "Experiments on ion cyclotron resonance," *The Physics of Fluids,* vol. 1, no. 5, pp. 446--451, 1958.

[5] N. J. Fisch, "Confining a tokamak plasma with rf-driven currents," *Physical Review Letters,* vol. 41, no. 13, p. 873, 1978.

[6] N. J. Fisch, "Theory of current drive in plasmas," *Reviews of Modern Physics,* vol. 59, no. 1, p. 175, 1987.

[7] A. H. Reiman, "Suppression of magnetic islands by rf driven currents," *The Physics of Fluid,* vol. 26, no. 5, pp. 1338--1340, 1983.

[8] E. Westerhof, "Requirements on heating or current drive for tearing mode stabilization by current profile tailoring," *Nuclear fusion,* vol. 27, no. 11, p. 1929, 1987.

[9] F. F. Chen, Introduction to plasma physics, Springer Science \& Business Media, 2012.

[10] D. A. Mendis, H. L. Houpis and J. R. Hill, "The gravito-electrodynamics of charged dust in planetary magnetospheres," *Journal of Geophysical Research: Space Physics,* vol. 87, no. A5, pp. 3449--3455, 1982.

[11] R. J. Goldston and P. H. Rutherford, Introduction to plasma physics, 1st ed., London: IOP, 1997.

[12] H. W. Hendel, T. K. Chu and P. A. Politzer, "Collisional drift waves identification, stabilization, and enhanced plasma transport," *The Physics of fluids,* vol. 11, no. 11, pp. 2426-2439, 1968.

[13] T. C. Simonen, T. K. Chu and H. W. Hendel, "Feedback Control of Collisional Drift Waves by Modulated Parallel-Electron-Current Sink-Experiment and Interpretation," *Physical Review Letters,* vol. 23, no. 11, p. 568, 1969.

[14] B. D. Scott, "Free-energy conservation in local gyrofluid models," *Physics of Plasmas,* vol. 12, no. 10, p. 102307, 2005.

[15] R. F. Ellis, E. M. Marshall and R. Majeski, "Collisional drift instability of a weakly ionized argon plasma," *Journal of Plasma Physics,* vol. 22, no. 2, pp. 113-131, 1980.

[16] O. Grulke, S. Ullrich, T. Windisch and T. Klinger, "Laboratory studies of drift waves: nonlinear mode interaction and structure formation in turbulence," *Plasma Physics and Controlled Fusion,* vol. 49, no. 12B, p. 247, 2007.

[17] T. Kaneko, H. Tsunoyama and R. Hatakeyama, "Drift-wave instability excited by field-aligned ion flow velocity shear in the absence of electron current," *Physical review letters,* vol. 90, no. 12, p. 125001, 2003.

[18] F. F. Chen, "Universal'' Overstability of a Resistive, Inhomogeneous Plasma Physics of Fluids," *The Physics of Fluids,* vol. 8, no. 912, pp. 1323-1333, 1965.

[19] C. Z. Cheng and L. Chen, "Unstable universal drift eigenmodes in toroidal plasmas," *The Physics of Fluids,* vol. 23, no. 9, pp. 1770-1773, 1980.

[20] N. A. Krall and M. N. Rosenbluth, "Universal Instability in Complex Field Geometries," *The Physics of Fluids,* vol. 8, p. 1488, 1965.

[21] L. D. Pearlstein and H. L. Berk, "Universal Eigenmode in a Strongly Sheared Magnetic Field," *Physical Review Letters,* vol. 23, p. 220, 1969.

[22] D. W. Ross and S. M. Mahajan, "Are drift-wave eigenmodes unstable?," *Physical Review Letters,,* vol. 40, no. 5, p. 324, 1978 .

[23] K. Tsang, P. Catto, J. Whitson and J. Smith, "Absolute Universal Instability" Is Not Universal," *Physical Review Letters,* vol. 40, no. 5, p. 327, 1978.

[24] C. Z. Cheng and L. Chen , "Unstable universal drift eigenmodes in toroidal plasmas," *The Physics of Fluids,* vol. 23, no. 9, pp. 1770--1773, 1980.

[25] N. D'angelo and N. Rynn, "Diffusion and recombination of a highly ionized cold plasma in a magnetic field," *The Physics of Fluids,* vol. 4, p. 1303, 1961.

[26] S. S. Moiseev and R. Z. Sagdeev, "The theory of the stability of non-uniform plasma and anomalous diffusion," *Sov. Phys. - JETP,* vol. 44, p. 515–517, 1963.

[27] D. Jukes, "Micro-instabilities in magnetically confined, inhomogeneous plasma.," *The Physics of Fluids,* vol. 7, p. 1468–1474, 1964.

[28] F. F. Chen, "Normal Modes for Electrostatic Ion Waves in an Inhomogeneous Plasma," *The Physics of Fluids,* vol. 7, no. 7, p. 949, 1964.

[29] F. F. Chen, "Universal overstability of a resistive, inhomogeneous plasma," *The Physics of Fluids,* vol. 8, no. 7, p. 1323–1333, 1965.

[30] H. Lashinsky, "Universal Instability in a Fully Ionized Inhomogeneous Plasma," *Physical Review Letters,* vol. 12, no. 5, p. 121, 1964.

[31] H. W. Hendel, T. K. Chu and P. A. Politzer, "Collisional Drift Waves—Identification, Stabilization, and Enhanced Plasma Transport," *The Physics of Fluids,* vol. 11, p. 2426, 1968.

[32] R. F. Ellis and R. W. Motley, "Collisional Drift Instability Driven by an Axial Current," *Physical Review Letters,* vol. 27, p. 1496, 1971.

[33] T. K. Chu, B. Coppi, H. W. Hendel and F. W. Perkins, "Drift Instabilities in a Uniformly Rotating Plasma Cylinder," *The Physics of Fluids,* vol. 12, p. 203, 1969.

[34] R. F. Ellis and E. Marden Marshall, "Comparison of local and nonlocal theories of the collisional drift instability," *The Physics of Fluids,* vol. 22, no. 11, p. 2137, 1979.

[35] E. M. Marshall, R. F. Ellis and J. E. Walsh, "Collisional drift instability in a variable radial electric field," *Plasma physics and controlled fusion,* vol. 28, no. 98, p. 1761, 1986.

[36] W. Horton, "Drift waves and transport," *Reviews of Modern Physics,* vol. 71, no. 3, p. 735, 1999.

[37] P. A. Politzer, "Drift instability in collisionless alkali metal plasmas," *The Physics of Fluids,* vol. 14, no. 11, pp. 2410-2425, 1971.

[38] K. I. Thomassen, "Feedback stabilization in plasmas," *Nuclear Fusion,,* vol. 11, p. 175, 1971.

[39] V. V. E. Arsenin and V. A. & Chuyanov, "Suppression of plasma instabilities by the feedback method," *Soviet Physics Uspekhi,,* vol. 20, no. 9, p. 736–762, 1977.

[40] H. W. Hendel, T. K. Chu, P. F. W. and T. C. Simonen, "Remote Feedback Stabilization of Collisional Drift Instability by Modulated Microwave Energy Source," *Physical Review Letters,,* vol. 24, no. 3, p. 90, 1970.

[41] P. W. Terry, "Suppression of turbulence and transport by sheared flow," *Reviews of Modern Physics,* vol. 72, no. 1, p. 109, 2000.

[42] A. Simon, "Instability of a Partially Ionized Plasma in Crossed Electric and Magnetic Fields," *The Physics of Fluids,* vol. 6, no. 3, p. 382–388, 1963.

[43] F. Hoh, "Instability of penning-type discharges," *Physics of Fluids,* vol. 6, p. 1184–1191, 1963.

[44] N. A. Kral and M. N. Rosenbluth, "Universal Instability in Complex Field Geometries," *The Physics of Fluids,* vol. 8, p. 1488, 1965.

[45] B. .. Coppi, "Current-Driven Instabilities in Configurations with Sheared Magnetic Fields," *The Physics of Fluids,* vol. 8, p. 2273, 1965.

[46] k. Kitao, "Effects of Magnetic Shear on Density Gradient Drift Instabilities," *Zeitschrift f Naturforschung A,* vol. 22, no. 11, pp. 1689--1700, 1967.

[47] R. J. Groebner, K. H. Burrell and R. P. Seraydarian, "Role of edge electric field and poloidal rotation in the L-H transition," *Physical review letters,* vol. 64, no. 25, p. 3015, 1990.

[48] T. R. Desjardins, Dynamics of turbulence and flows in a helicon plasma under electrode biasing, The University of New Mexico, 2016.

[49] M. A. Pedrosa , C. Hidalgo, E. Calderón, T. Estrada, A. Fernández, J. Herranz and I. Pastor, "Threshold for sheared flow and turbulence development in the TJ-II stellarator," *Plasma Physics and Controlled Fusion,* vol. 47, no. 6, p. 777, 2005.

[50] K. H. Burrell , "Effects of E X B velocity shear and magnetic shear on turbulence and transport in magnetic confinement devices," *Physics of Plasmas,* vol. 4, no. 5, pp. 1499--1518, 1997.

[51] Y. C. Saxena and P. I. John, "Dispersion and spectral characteristics of crossfield instability in collisional magnetoplasma," *Pramana,* vol. 8, no. 2, pp. 123--132, 1977.

[52] S. Sen, M. G. Rusbridge and R. J. Hastie, "Collisionless drift waves in the H mode edge," *Nuclear fusion,* vol. 34, no. 1, 1994.

[53] C. D. Vore, "Current-driven resistive drift instabilities in sheared magnetic fields," *Nuclear Fusion,* vol. 21, no.1, p. 105, 1981.

[54] R. Bharuthram, M. A. Hellberg, and R. D. Lee, "The cross field current-driven ion-acoustic instability in a collisional plasma," *Theoretical Nuclear Physics,* vol. 28, no. 1, pp. 267--279, 1982.

[55] M. Gregoire and P. Rolland , "Shear stabilization of drift dissipative instabilities," *Nuclear Fusion,* vol. 13, no. 6, p. 867, 1973.

[56] C. L. Chang, J. F. Drake, N. T. Gladd and C. S. Liu , "Unstable dissipative drift modes in a sheared magnetic field," *The Physics of Fluids,* vol. 23, no. 10, pp. 1998--2006, 1980.

[57] J. Bodo, D. Gray, S. Jachmich, R. Conn and G. P. Terry, "Enhanced particle confinement and turbulence reduction due ...," *Nuclear Fusion,* vol. 40, p. 1397, 2000.

[58] S. Khrapak and V. Yaroshenko, "Ion drift instability in a strongly coupled collisional complex plasma," *Plasma Physics and Controlled Fusion,* vol. 62, no. 10, 2020.

[59] Y. V. Esipchuk and G. N. Tilinin, "Drift instability in a Hall-current plasma accelerator," *Sov. Phys. - Tech. Phys,* vol. 21, 1976.

[60] P. J. Catto, M. Rosenbluth and C. S. Liu, "Parallel velocity shear instabilities in an inhomogeneous plasma with a sheared magnetic field," *The Physics of Fluids,* vol. 16, no. 10, pp. 1719--1729, 1973.

[61] J. D. Hubba , S. L. Ossakow, P. Satyanarayana and P. N. Guzdar, "Linear theory of the E x B instability with an inhomogeneous electric field," *Journal of Geophysical Research: Space Physics,* vol. 88, no. A1, pp. 425-434, 1983.

[62] S. Ku, J. Abiteboul, P. H. Diamond, G. Dif-Pradalier, J. M. Kwon, Y. Sarazin, T. S. Hahm, X. Garbet, C. S. Chang and G. Latu, "Physics of intrinsic rotation in flux-driven ITG turbulence," *Nuclear Fusion,* vol. 52, no. 6, p. 063013, 2012.

[63] R. L. Tanna, H. Raj, G. Ghosh, R. Kumar, S. Aich, T. Macwan, D. Kumawat and K. A. Jadeja, "Overview and operation and experiments in the Aditya-U tokamak," *Nuclear Fusion,* vol. 59, p. 112006, 20019.

[64] T. Ohkawa and R. L. Miller, "Creation of localized sheared flow by ion trapping.," *Physics of Plasmas,* vol. 12, p. 094506, 2005.

[65] I. Romadanov, A. Smolyakov, Y. Raitses, I. Kaganovich, T. Tian and S. Ryzhkov, "Structure of nonlocal gradient-drift instabilities in Hall E × B discharges," *Physics of Plasmas,* vol. 23, no. 12, 2016.

[66] M. Okabayashi and V. Arunasalam., "Creation of localized sheared flow by ion trapping," *Physics of Plasmas,* vol. 12, no. 9, p. 094506, 2005.

[67] W. Tang, R. White and P. Guzdar, "Impurity effects on ion-drift-wave eigenmodes in a sheared magnetic field," *The Physics of Fluids,* vol. 23, no. 1, pp. 167-173, 1980.

[68] J. C. Perez and W. Horton, "Drift wave instability in the Helimak experiment," *Physics of Plasmas,* vol. 13, p. 032101, 2006.

[69] A. Brekke, Physics of the upper polar atmosphere, Springer Science & Business Media, 2012.

[70] R. Schunk and . A. Nagy, Ionospheres: physics, plasma physics, and chemistry, Cambridge university press, 2009.

[71] J. V. Sickle, "GPS for Land Surveyors," [Online]. Available: https://www.e-education.psu.edu/geog862/node/1715.

[72] G. Paschmann, S. Haaland, . T. Rudolf and A. T. Rudolf A. Treu, Auroral plasma physics, Springer Science & Business Media, 2003.

[73] M. Zettergren, "Ionospheric plasma transport and loss in auroral downward current regions," *Journal of Geophysical Research: Space Physics,* vol. 117, no. A6, 2012.

[74] J. D. Huba, N. T. Gladd and K. Papadopoulos, "Lower-hybrid-drift wave turbulence in the distant magnetotail," *Geophysical Research Letters,* vol. 83, no. A11, pp. 5217-5226, 1978.

[75] P. B. Hays, R. A. Jones and M. H. Rees, "Auroral heating and the composition of the neutral atmosphere," *Planetary and Space Science,* vol. 21, no. 4, pp. 559-573, 1973.

[76] M. L. Duboin and Y. Kamide, "Latitudinal variations of Joule heating due to the auroral electrojets," *JGR: Space Physics,* vol. 89, no. A1, pp. 245-251, 1984.

[77] W. D. Jones, A. Lee, S. M. Gleman and H. J. Doucet, "Propagation of ion-acoustic waves in a two-electron temperature plasma," *Physical ReviewLetters,* vol. 35, p. 1349, 1975.

[78] M. Y. Yu and P. Shukla, "Linear and nonlinear modified electron-acoustic waves," *Journal of Plasma Physics,* vol. 29, no. 3, pp. 409-413., 1983.

[79] A. J. Lichtenberg and H. Meuth, "Hot-electron instability in mirror geometry.," *The Physics of fluids,* vol. 29, no. 11, pp. 3511-3514, 1986.

[80] N. Yasushi and T. Nagasawa, "Excitation of ion-acoustic rarefactive solitons in a two-electron-temperature plasma," *The Physics of fluids,* vol. 29, no. 2, pp. 345-348, 1986.

[81] M. Bose and S. Guha, "Electron acoustic and lower hybrid drift dissipative instabilities in a multi-ion species plasma," *Physica Scripta,* vol. 34, no. 1, p. 63, 1986.

[82] S. V. Singh, R. V. Reddy and G. S. Lakhina, "Modulational instability of electron-acoustic waves in the auroral region," in *Proceedings of the ILWS Workshop*, 2006.

[83] P. H. Sakanaka and R. d. Trindade Faria , "Evolution of Electron-Acoustic Wave in Auroral Region.," in *In AIP Conference Proceedings*, 2003.

[84] p. Bala and T. S. Gill, "Multimode excitation and modulational instability of beam plasma system with Tsallis-distributed electrons," *Pramana,* vol. 95, no. 2, pp. 1-14, 2021.

[85] V. I. Arefev , *Sov.Phy.Tech.Phys,* vol. 14, p. 1487, 1970.

[86] M. Mohan and M. Y. Yu, "Drift dissipative instabilities of electron-acoustic and lower-hybrid waves," *Journal of Plasma Physics,* vol. 29, no. 1, p. 127, 1983.

[87] J. E. Willett and Y. Aktas , "Drift dissipative instabilities between the electron and ion cyclotron frequencies," *Journal of Applied Physics,* vol. 59, no. 8, p. 2985, 1986.

[88] A. Kuley and V. K. Tripathi, , "Stabilization of ion temperature gradient driven modes by lower hybrid wave in a tokamak," *Physics Of Plasmas,* vol. 16, no. 3, p. 032045, 2009.

[89] W. Horton, D. I. Choi and W. M. Tang , "Toroidal drift modes driven by ion pressure gradients," *The Physics of Fluids,* vol. 24, no. 6, pp. 1077-1085, 1981.

[90] B. Coppi and F. Pegoraro, "Theory of the ubiquitous mode," *Nuclear Fusion,* vol. 17, no. 5, p. 969, 1977.

[91] M. N. Rosenbluth, R. D. Hazeltine and F. L. Hinton, "Plasma transport in toroidal confinement systems}," *Physics of Fluids,* vol. 15, no. 1, p. 15 116, 1972.

[92] J. Wesson, Tokamak, Clarendon press, Oxford, 1987.

[93] S. I. Braginskii and M. A. Leontovich, "Reviews of plasma physics," Consultants Bureau New York, 1965.

[94] M. A. Beer and G. W. Hammett, "Toroidal gyrofluid equations for simulations of tokamak turbulence," *Physics of Plasmas,* vol. 3, no. 11, p. 4046–4064, 1996.

[95] S. Brunner, S. Fivaz, T. M. Tran T M and J. Vaclavik, "Global approach to the spectral," *Physics of Plasma,* vol. 5, no. 11, p. 3929–3949, 1998.

[96] B. B. Kadomtsev and O. P. Pogutse , "Theory of Beam-Plasma Interaction," *Physics of Fluids,* vol. 14, no. 11, pp. 2470-2475, 1971.

[97] A. Sen and A. K. Sundaram, "Ballooning stability of a toroidally rotating plasma," *Nuclear Fusion,* vol. 29, no. 7, p. 1161, 1989.

[98] G. G. Craddock and P. H. Diamond, "Theory of shear suppression of edge turbulence by externally driven radio-frequency waves," *Physical Review Letters,* vol. 67, p. 1535, 1991.

[99] G. Ciraolo, F. Briolle, C. Chandre, E. Floriani, R. Lima, M. Vittot, M. Pettini, C. Figarella and P. Ghendrih, "Control of Hamiltonian chaos as a possible tool to control anomalous transport in fusion plasmas," *Physical Review E,* vol. 69, p. 056213, 2004.

[100] J. Chen and Z. Gao, "Tokamak Plasma Flows Induced by Local RF Forces," *Plasma Science and Technology,* vol. 7, no. 10, pp. 809-816, 2015.

[101] W. Horton, "Drift waves and transport," *Reviews of Modern Physics,* vol. 71, no. 3, p. 735, 1999.

[102] L. I. Rudakov and R. J. Sagdeev, "On the Instability of a Nonuniform Rarefied Plasma in a Strong Magnetic Field}," *Soviet Physics Doklady,* vol. 6, p. 415, 1961.

[103] B. Coppi, M. N. Rosenbluth and R. Z. Sagdeev, "Instabilities due to temperature gradients in complex magnetic field configurations," *The Physics of Fluids,* vol. 10, no. 3, p. 582, 1967.

[104] A. K. Sen, B. Song and J. Chen, "Summary of ion temperature gradient instability studies in the Columbia linear machine," *Physica Scripta,* vol. 52, no. 4, p. 467, 1995.

[105] W. Horton, D. I. Choi and B. G. Hong, "Electromagnetic drift modes driven by pressure gradients in tokamaks," *Physics of Fluids,* vol. 26, no. 4, pp. 1461-1466, 1983.

[106] P. N. Guzdar, L. Chen, W. M. Tang and P. H. Rutherford, "Ion-temperature-gradient instability in toroidal plasmas," *The Physics of Fluids,* vol. 26, pp. 673-677, 1983.

[107] N. Ahmad and M. Ahmad, "Parametric Instability of a Lower Hybrid Wave in Two Ion Species plasma," *Research and reviews: journal of Pure and Applied Physics,* vol. 4, no. 2, pp. 35-41, 2016.

[108] H. Biglari, P. H. Diamond and M. N. Rosenbluth, "Toroidal ion-pressure-gradient-driven drift instabilities and transport revisited," *Physics of Fluids B,* vol. 1, no. 1, pp. 109-118, 1989.

[109] D. Jovanovic and W. Horton, "Impurity effects on linear and nonlinear ion-temperature-gradient-driven modes," *Physics of Plasmas,* vol. 2, no. 5, p. 1561, 1995.

[110] A. Jarmen, P. Andersson and J. Weiland, "Fully Toroidal IonTemperatureGradient Driven Drift Modes," *Nuclear Fusion,* vol. 27, no. 6, p. 941, 1987.

[111] I. Sandberg, H. Isliker, V. P. Pavlenko, K. Hizanidis and K. Vlahos, "Fluid simulations of toroidal ion temperature gradient turbulence," *Physics of Plasmas,* vol. 13, p. 022311, 2006.